american physiological society

JNP JOURNAL OF NEUROPHYSIOLOGY

J Neurophysiol 126: 1723–1739, 2021.
First published October 13, 2021; doi:10.1152/jn.00320.2021

RESEARCH ARTICLE

Neuroscience of Disease

Inducing neuroplasticity through intracranial θ-burst stimulation in the human sensorimotor cortex

Jose L. Herrero,[1,2] Alexander Smith,[2] Akash Mishra,[1,2] Noah Markowitz,[1,2] Ashesh D. Mehta,[1,2] and Stephan Bickel[1,2,3]

[1]*The Feinstein Institutes for Medical Research, Northwell Health, Manhasset, New York;* [2]*Department of Neurosurgery, Zucker School of Medicine at Hofstra/Northwell, Manhasset, New York; and* [3]*Department of Neurology, Zucker School of Medicine at Hofstra/Northwell, Manhasset, New York*

Abstract

The progress of therapeutic neuromodulation greatly depends on improving stimulation parameters to most efficiently induce neuroplasticity effects. Intermittent θ-burst stimulation (iTBS), a form of electrical stimulation that mimics natural brain activity patterns, has proved to efficiently induce such effects in animal studies and rhythmic transcranial magnetic stimulation studies in humans. However, little is known about the potential neuroplasticity effects of iTBS applied through intracranial electrodes in humans. This study characterizes the physiological effects of intracranial iTBS in humans and compare them with α-frequency stimulation, another frequently used neuromodulatory pattern. We applied these two stimulation patterns to well-defined regions in the sensorimotor cortex, which elicited contralateral hand muscle contractions during clinical mapping, in patients with epilepsy implanted with intracranial electrodes. Treatment effects were evaluated using oscillatory coherence across areas connected to the treatment site, as defined with corticocortical-evoked potentials. Our results show that iTBS increases coherence in the β-frequency band within the sensorimotor network indicating a potential neuroplasticity effect. The effect is specific to the sensorimotor system, the β band, and the stimulation pattern and outlasted the stimulation period by ∼3 min. The effect occurred in four out of seven subjects depending on the buildup of the effect during iTBS treatment and other patterns of oscillatory activity related to ceiling effects within the β band and to preexistent coherence within the α band. By characterizing the neurophysiological effects of iTBS within well-defined cortical networks, we hope to provide an electrophysiological framework that allows clinicians/researchers to optimize brain stimulation protocols which may have translational value.

NEW & NOTEWORTHY θ-Burst stimulation (TBS) protocols in transcranial magnetic stimulation studies have shown improved treatment efficacy in a variety of neuropsychiatric disorders. The optimal protocol to induce neuroplasticity in invasive direct electrical stimulation approaches is not known. We report that intracranial TBS applied in human sensorimotor cortex increases local coherence of preexistent β rhythms. The effect is specific to the stimulation frequency and the stimulated network and outlasts the stimulation period by ∼3 min.

β oscillations in sensorimotor cortex; direct electrical brain stimulation; intracranial EEG; iTBS; neuronal plasticity

INTRODUCTION

Brain stimulation therapies such as transcranial magnetic stimulation (TMS) and direct electrical stimulation (DES) of subcortical and cortical structures are increasingly used to treat neurological and psychiatric disorders such as movement disorders (1), epilepsy (2, 3), Tourette's syndrome (4), and major depressive (5, 6) and obsessive compulsive disorders (7), and they are actively being studied for use in stroke recovery (8), posttraumatic stress disorder (PTSD) (9), and substance abuse disorders (10, 11). In DES [including deep brain stimulation (DBS) and direct cortical stimulation (DCS)], the therapeutic effect is thought to be related to acutely enhancing or inhibiting activity in specific brain regions, and until recently, less emphasis was placed on the potential contributing role of neural plasticity induced by

Correspondence: J. L. Herrero (jherreroru@northwell.edu); S. Bickel (Sbickel@northwell.edu).
Submitted 13 July 2021 / Revised 20 September 2021 / Accepted 8 October 2021

electrical stimulation. Despite the important role of neural plasticity as part of the therapeutic effects in DES (12–14), there is still much to be learned about the most effective plasticity-inducing stimulation parameters using this approach (15).

Noninvasive stimulation modalities such as repetitive TMS (rTMS) can cause systematic changes in cortical excitability (16). In seminal studies, high-frequency rTMS (>5 Hz) applied to the motor cortex caused increased cortical excitability as measured by the amplitude of motor-evoked potentials (MEP) in contrast to low-frequency (~1 Hz) stimulation that more frequently led to an opposite effect (16–18). Although rTMS is currently used to treat a wide range of clinical conditions, recent studies have shown that TMS-induced plasticity effects are transient, require repeated treatment visits, and suffer from a wide interindividual variability, being effective in ~30% of patients (18, 19). Thus, the addition of potential anatomical targets and its portability renders DES as a valid treatment option in certain patient populations despite its invasiveness (2, 20).

A recent trial that tested the high-frequency rTMS-like stimulation applied directly to the brains of individuals with intracranially implanted electrodes found neuroplasticity effects in functionally connected brain areas (21). This DCS trial demonstrated subject-dependent and site-dependent responses (enhancement or suppression) that could not be predicted by the characteristics of the stimulation frequency alone. A potential explanation of the heterogenous effects is that stimulation was applied across several different functional regions across patients. In addition, the authors used intermittent α-frequency stimulation, whereas the most efficient rTMS protocol to induce increases in neural excitability uses intermittent θ-burst stimulation (iTBS, brief bursts of 50–100 Hz, pulses repeated at 5 Hz) (18, 22–28).

In our study, we directly applied iTBS to one specific network, the sensorimotor network (iTBS-DCS) and assessed the treatment effects exclusively on connected sites as defined by corticocortical-evoked potentials (CCEPs) (29–33). The treatment sites were carefully selected based on clinical functional stimulation mapping results in seven patients that had extensive sensorimotor cortical coverage. Based on the known prominence of β oscillations in the sensorimotor system, as a read-out of the effect, we measured changes in β coherence across the sensorimotor network, as well as changes in effective connectivity using CCEPs (similar to Ref. 21) during the periods preceding and succeeding the treatments. We report results that might guide further investigations in the design of DCS protocols aiming at inducing neuroplasticity in cortical networks.

METHODS

Patient Selection

Seven patients with medically intractable epilepsy who underwent electrode implantation at North Shore University (6) or Lenox Hill (1) hospitals for seizure localization were enrolled in the study. The decision to implant, the electrode targets, and the duration of implantation were made entirely on clinical grounds. The patients had sensorimotor electrode coverage because the clinical hypothesis included a potential involvement of these areas in the seizure network. Patient characteristics are described in Table 1. Patients were selected on the bases of having *1*) ample electrode coverage of sensorimotor areas; *2*) contralateral hand and/or arm motor contractions upon clinical high-frequency stimulation mapping (HFSM), and *3*) confirmed seizure onset focus outside sensorimotor areas. All patients provided informed written consent according to a protocol approved by the local Institutional Review Board following the Declaration of Helsinki. Patients were informed that participation in this study would not alter their clinical care and that they could withdraw from the study without jeopardizing their care. Patients were also informed that this study had no direct implications to treat their epilepsy. Three patients in this study were included in a prior study (34). However, the evaluations put forth here are unique to this study, as they refer to different stimulation sessions and stimulation parameters. Stimulation sessions took place after enough seizures were captured for clinical purposes and antiepileptic drugs (AEDs) were restarted (Table 1).

Electrode Registration

Our electrode registration method was previously described in detail (35). Briefly, we used the iELVis toolbox, which makes use of BioImage Suite, FSL, FreeSurfer, and custom-written code for intracranial electrode localization. The electrode contacts are semi-manually located in the postimplantation CT which is coregistered to the preimplantation MRI. In addition, FreeSurfer aligns the patient's preimplantation MRI to a standard coordinate space, automatically parcellating the brain and assigning anatomical regions to each contact. Finally, iELVis software is used to project the contacts locations onto FreeSurfer's standard image.

Electrophysiological Recording and Preprocessing

Intracranial electrographic (iEEG) signals were acquired continuously at 512 Hz or 3 kHz using a clinical recording system (Xltek Quantum 256, Natus Medical) or a Tucker Davis PZ5M module (TDT). iEEG data were extracted by bandpass filtering (8-pole Butterworth filter, cutoffs at 0.01 and 250 Hz). Either subdural or skull electrode contacts were used as references, depending on recording quality at the bedside, and were subsequently re-referenced to a common average. The signal quality and their power spectra were inspected online using interactive oscilloscope tools (TDT Synapse) and standard MATLAB functions (pwelch and spectrogram) before the experiment started to ensure their physiological properties.

High-Frequency Stimulation Mapping

HFSM is a clinical functional mapping technique to localize seizure onset (and eloquent) areas, which is performed in patients implanted with intracranial electrodes after anticonvulsant medications are resumed. A Grass S12D (Grass Technologies) or a Tucker Davis (IZ2MH) stimulator was used to apply bipolar stimulation with biphasic matched-square wave pulses (100 μs or 200 μs/phase) and current amplitudes ranging from 0.5 to 4 mA or 0.5 to 10 mA for depth and subdural electrodes, respectively, at a rate of 50

Table 1. *Summary of patients and stimulation characteristics*

Patient ID	Age	Sex	Handedness	Implant Type	Treatment Location (Current Amplitude)	Total Contacts (*CCEPs)	HFSM Effect	Seizure Focus	AED
1	49	F	R	sEEG (bilateral)	Left M1 (1.2 mA)	247 (13)	Fingers/elbow/shoulder muscle contractions	Bilateral mesial temporal lobes	Clonazepam Lamotrigine
2	29	M	R	sEEG (left)	Left M1-S1 (0.5 mA)	220 (15)	Thenar muscle contraction and clonic fingers movement	Left posterior perilesional, superior posterior temporal operculum, and left posterior insula	Lamotrigine Topiramate Clobazam
3	48	M	R	sEEG (bilateral)	Right M1-S1 (1 mA)	350 (9)	Thenar muscle contraction and elbow contraction	Right posterior mid-lateral temporal region (fusiform and lingual gyri)	Clobazam Clonazepam Perampanel Cenobamate
4	37	F	R	sEEG (bilateral)	Right M1-S1 (0.9 mA)	152 (11)	Clonic fingers movement	Left mesial temporal lobe	Felbamate Perampanel Primidone*
5	32	F	R	sEEG (bilateral)	Right S1 (1.1 mA)	189 (10)	Clonic fingers movement	Right superior temporal gyrus and most of Sylvian fissure	Carbamazepine Levetiracetam
6	20	M	R	Grids/strips (right)	Right M1-S1 (2.2 mA)	163 (26)	Clonic fingers movement, wrist pronation	Right hippocampus, right amygdala, mesial cortical lesion posterior to right hippocampus	Lacosamide Levetiracetam
7	56	F	L	sEEG (left)	Left S1 (1.35 mA)	136 (11)	Finger/hand/elbow/biceps muscle contraction	Left amygdala, left hippocampus, left inferior temporal lobe (rarely)	Carbamazepine Levetiracetam

High-frequency stimulation mapping (HFSM): clinical procedure during which every electrode contact pair is stimulated with high-frequency stimulation bursts to determine function. All HFSM-related motor contractions were contralateral to the stimulation site. Treatment locations for iTBS/i8Hz were selected based on HFSM results (contact pairs that elicited the most specific finger/arm contractions) and the final current for the subsequent treatment was set at an intensity of 80% of the motor threshold. Treatment locations: M1, primary motor cortex (both stimulation contacts were immediately anterior to the central sulcus); S1, primary somatosensory cortex (both stimulation contacts were immediately posterior to the central sulcus); M1-S1, sensorimotor cortex (paracentral, one stimulation contact was anterior to the central sulcus and the other posterior to it). Total contacts: total number of electrode contacts recorded and total number of contacts with significant CCEPs located in gray matter (white matter and cerebrospinal fluid contacts were discarded). Seizure focus: all seizure onset foci were outside sensorimotor areas. Antiepileptic drugs (AEDs) taken during treatments (iTBS and i8Hz). Primidone* taken only during HFSM. CCEPs, corticocortical-evoked potentials; F, female; i8Hz, intermittent α-burst stimulation; iTBS, intermittent θ-burst stimulation; L, left; M, male; R, right; sEEG, stereo EEG.

Hz up to 0.5–2 s duration. All seven patients included in this study had HFSM of sensorimotor cortical sites which elicited contralateral clonic or tonic-clonic muscle contractions (36) (Table 1 and Fig. 1).

Treatment Site Selection and Stimulation Protocol

As treatment sites, we selected electrode contacts in which high-frequency (50 Hz, ~1-s duration) stimulation trains applied during HFSM elicited the most specific contralateral finger or hand movements (Table 1) at the lowest current amplitude in 5 out of 10 consecutive trials in which the target muscle was relaxed (e.g., resting motor threshold; 37–39). To minimize variability across patients the preferred stimulation site was the hand area of the motor cortex (Fig. 1*A*). However, sites of electrode implantation were based on clinical criteria, and not every patient had electrodes implanted within the hand area. In these cases, the closest region to the hand motor cortex that elicited finger, wrist, or arm movements was selected. Treatment stimulation currents matching 80% of the motor threshold were used as in previous studies (17, 40), and no epileptiform after-discharges occurred at these intensities. iTBS in TMS studies consists of three pulses delivered at 50 Hz (20-ms separating each pulse), and each set of three pulses is repeated at 5 Hz (Fig. 2, *inset*). In our iTBS protocol, we applied this sequence of pulses for 2 s (30 pulses/train) repeated every 10 s (8-s intertrain interval). Each pulse consisted of a bipolar, biphasic, square wave with 200 μs/phase. In the comparison condition (i8Hz), single stimulation pulses were administered at intervals of 125 ms for a period of 5 s (40 pulses/train) and repeated every 15 s (10-s intertrain interval). Similar stimulation frequencies ranging from 3 to 8 Hz were used in recent DBS studies (15, 41, 42). In our study, the number of total pulses was similar across treatment modalities (iTBS, 30 × 20 = 600 pulses; i8Hz, 40 × 15 = 600 pulses). Treatments were applied in a randomized order across subjects with a long (>45 min) interval between treatments to allow for the washout of any residual effects from the previous treatment. Resting-state activity immediately before and after each treatment was recorded to compute the coherence measures (Fig. 2, *inset*).

Corticocortical-Evoked Potentials

To localize brain areas connected to the treatment sites, we performed CCEP mapping (Fig. 3*A*) (31). CCEP mapping has been used to examine frontoparietal (30, 43), hippocampal (44), visual (45), language (32, 33, 46), and other networks (43). Single-pulse electrical stimulation [biphasic square-wave pulses (200 μs/phase)] were applied at the treatment site (200 pulses, 1-s interstimulation interval with a ±300-ms jitter). To get robust CCEPs, stimulation currents were set at 4 mA or just below the threshold that elicited movement. We also used CCEPs to probe for possible neuroplasticity effects and applied CCEP stimulation before and after treatment (iTBS or i8Hz, Fig. 2*B*). CCEP stimulation ended at least 15 min before treatment onset to avoid potential residual

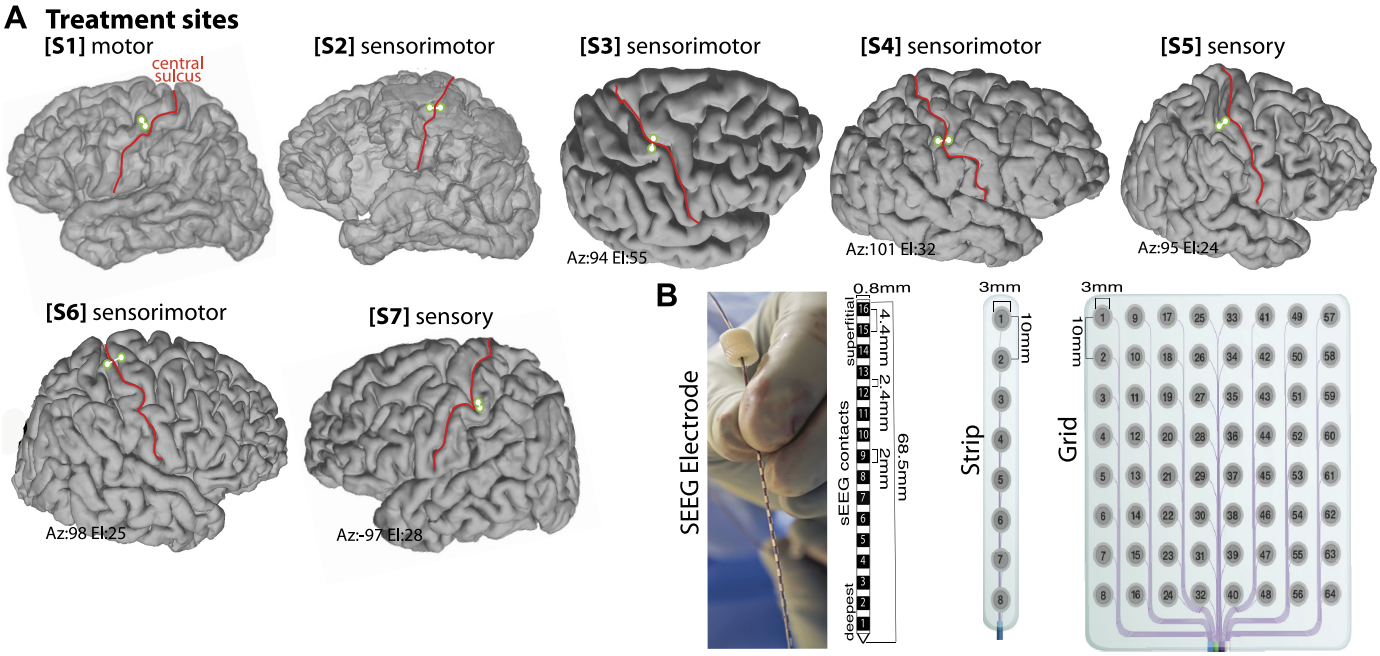

Figure 1. Treatment locations and recording electrodes. *A*: individual subjects' MRI and electrode contacts used for stimulation (treatment sites, green dots). High-frequency stimulation applied to these contacts during clinical mapping (before treatment) elicited contralateral clonic or tonic-clonic hand muscle contractions. All treatment sites were outside the seizure network. Connecting lines between contacts represent bipolar stimulation. *Subject 1* was stimulated in the motor cortex. *Subjects 2*, *3*, *4*, and *6* had 1 contact in the motor and the other in the sensory cortex. *Subjects 5* and *7* had both contacts in the sensory cortex. Red line, central sulcus. Some images were rotated to improve contacts' visibility. *B*: physical features of recording electrodes. *Left*: sEEG depth electrodes. *Right*: subdural strip and grid electrodes. sEEG, stereo EEG.

effects on neuronal excitability. Statistical significance of CCEPs was determined as follows: *1*) a bipolar montage (first spatial derivative) was applied to the data to reduce volume conduction effects; *2*) data from each electrode contact were epoched −1,000 to 1,000 ms centered on the electrical pulse; *3*) single CCEP traces were demeaned, baseline corrected (−200 to −25 ms), and averaged; *4*) the averaged CCEP trace was transformed to a t statistic by dividing the average at each timepoint by the standard error of the mean at the same timepoint. The absolute maximum of the t statistic during the poststimulus period (10–50 ms) was compared against the distribution of the t statistic during the

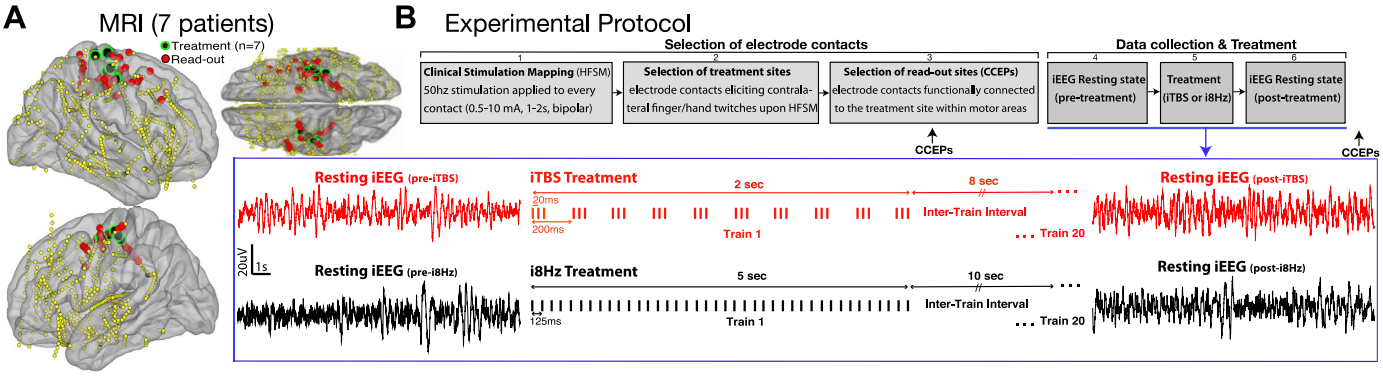

Figure 2. Treatment locations and experimental protocol. *A*: electrode contacts from 7 subjects registered onto a common brain surface. Treatment locations (green dots). Read-out electrode contacts (red dots) are connected to the treatment locations based on corticocortical-evoked potential (CCEP) mapping. Only sensorimotor contacts are shown here. *B*: experimental protocol. *Box 1*, high-frequency stimulation mapping (HFSM) reveals sites in sensorimotor cortex that elicit specific contralateral motor responses upon stimulation. *Box 2*, calculation of motor thresholds for each patient and sites of interest. A stimulated site eliciting the lowest threshold for motor response was chosen as the treatment site. *Box 3*, application of single pulses to treatment sites (>150 pulses, 4 mA, 200-μs pulse width) and selection of read-out sites (contacts connected to the treatment site) based on CCEP analyses (see *A*). *Box 4*, recording of intracranial EEG (iEEG) resting activity while subjects are awake but quiet and avoiding movements (2 min). *Box 5*, treatment is applied (either iTBS or i8Hz, see *inset*). *Box 6*, recording of iEEG resting activity immediately after treatment ends (2 min). Single pulses to treatment sites (~200 CCEPs) were also administered after the posttreatment resting period (black arrow) to assess potential treatment effects on CCEPs amplitude. *Inset*, *top*: iTBS treatment: three pulses of stimulation administered at 50 Hz repeat every 200 ms for a period of 2 s and an 8-s intertrain interval (2 s ON and 8 s OFF). Each 2-s iTBS train contains 30 pulses and repeats 20 times (30 × 20 = 600 pulses total). *Bottom*: i8Hz treatment: stimulation pulses administered at 8 Hz (1 pulse every 125 ms) for a period of 5 s (40 pulses per train) and a 10-s intertrain interval (5 s ON and 10 s OFF) and repeats 15 times (40 × 15 = 600 pulses total). i8Hz, intermittent α-burst stimulation; iTBS, intermittent θ-burst stimulation.

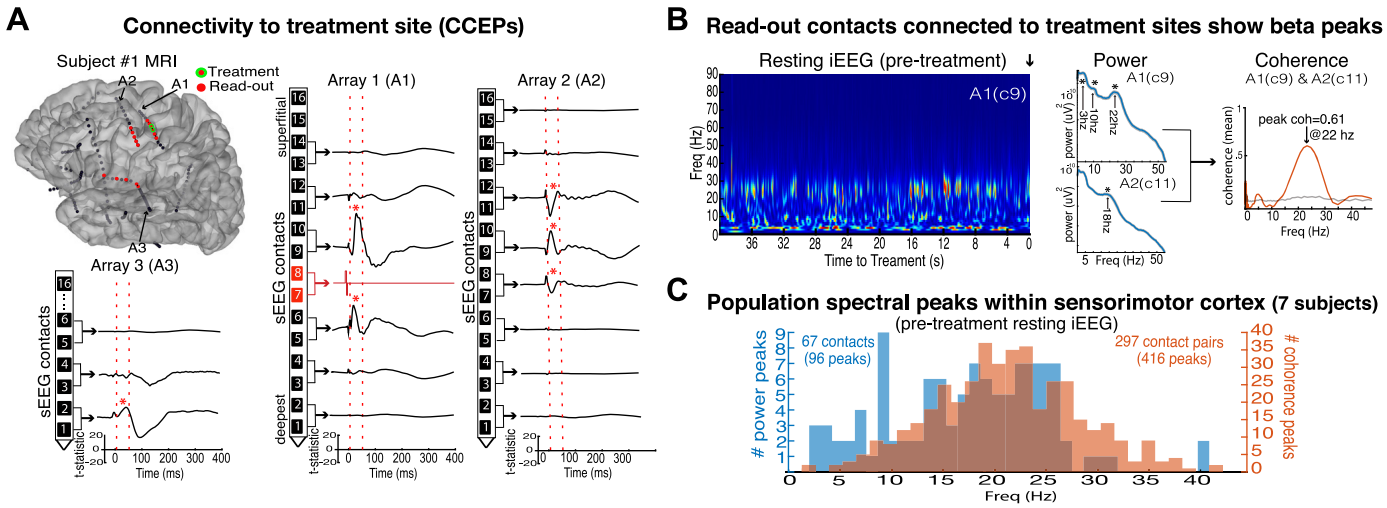

Figure 3. Areas connected to treatment sites have high β oscillations. *A*: connectivity to treatment sites using corticocortical-evoked potentials (CCEPs) in *subject 1*; single pulses (200 sweeps, bipolar stimulation, 4 mA) applied to the treatment site (*Array 1*, *contacts 7–8*, red line) elicit strong evoked potentials at nearby sites within sensorimotor cortex (*A1*, *contacts 5–10* and *A2*, *contacts 7–12*) and at more distant sites (*A3* with *contacts 1–4* located in the insula and other more distant contacts located in the most lateral portion of the sensorimotor cortex). Asterisks mark contacts with significant CCEPs (P1 peak amplitude >6 SD *t* statistic). Vertical dashed lines (red); analyses window (10–50 ms poststimulation). *B*, *left*: time-frequency power spectrum of one example electrode contact located in the motor cortex adjacent to the treatment site (*A1*, c9) during a 2-min resting period recorded before treatment. *Center*: averaged spectrograms show prominent spectral peaks in the β band for the same contact (*top*, ~22 Hz peak) and another contact adjacent to it (*bottom*, 18 Hz peak). *Right*: coherence between these two contacts (orange line, mean coherence across all overlapping windows; gray line pointwise significance level, α = 0.05). *C*: population spectral peaks (67 electrode contacts) and coherence peaks (297 contact pairs) of connected sites based on CCEP mapping within the sensorimotor cortex across all patients; power peaks (blue bars, 96 peaks from 67 contacts) and coherence peaks (orange bars, 416 peaks from 297 contacts). coh, Coherence; Freq, frequency; iEEG, intracranial EEG; sEEG, stereo EEG.

prestimulus baseline period. If the poststimulus *t* statistic was higher than 6 standard deviations, the response was considered as significant. These thresholds (6 SD) and time windows (10–50 ms, when the most direct synaptic effects occur) were based on prior studies (29, 44). Significant electrode contacts were considered as read-out contacts in which treatment effects were later evaluated. Read-out contacts outside gray matter (in white matter and cerebrospinal fluid) were discarded from the main analyses of treatment effects.

Coherence and Power Analyses

Analyses were conducted using the FieldTrip toolbox (47) and custom MATLAB scripts. After determining the sites of interest using CCEPs (e.g., contacts functionally connected to the treatment site, Figs. 2*A* and 3*A*), we applied a sensor-based analysis to these contacts: coherence was first calculated between all contacts showing significant CCEPs to the stimulation contact and then averaged across each pair combination. Stimulation contacts were discarded due to artifacts or low signal-to-noise ratio. Given the caution against the use of bipolar EEG for synchronization analyses (48–50), we used common average reference montage for our coherence analyses. To calculate the coherence between two iEEG contacts, we squared the magnitude of the cross spectrum of their raw signals, normalized it by the power spectra of each signal at each respective frequency, and smoothed it (51). The imaginary part of the coherence was used for the analysis, as it might be less impacted by common input sources (52). Each 2-min data set (e.g., pretreatment) was divided into overlapping 10-s windows (1/10 = 0.1-Hz resolution, sliding 2 s at a time), and windows with outliers (>4 SD of the mean coherence across all sliding windows) were discarded. The total windows discarded across all subjects were 0.8%. Statistical significance of dominant spectral coherence peaks was evaluated using cluster-based nonparametric tests implemented in Fieldtrip (see Fig. 3*C*, population coherence peaks). iEEG signals between contact pairs were shuffled (1,000 iterations), and the critical levels of the Wilcoxon–Mann–Whitney tests at each frequency were computed (see Fig. 3*B*, coherence plot for an example site, gray line shows pointwise significance level, α = 0.05, jackknife method). The dominant peaks in the power spectrum were determined using power spectral density estimates implemented in "periodogram.m" (95% confidence bounds, 4-s rectangular data windows, 2-s sliding). Very similar results were found using different window lengths (3 s or 5 s) and a frequency-dependent time-window analysis implemented in ft_freqanalysis.m (10-cycles time window for all frequencies with sliding Hanning tapers). Figure 3*B* shows single-electrode power plot examples and Fig. 3*C* shows the population power peaks. To assess whether the coherence between iTBS/i8Hz pre- and post-treatment was significantly different for any given contact pair (and at what specific frequencies), we used the nonparametric Monte Carlo test implemented in "ft_freqstatistics.m" at α level 0.01 (Fig. 4*A*, red line above *x*-axis). The peak coherence values at the β band (12–30 Hz) for all sensorimotor contact pairs combinations were extracted and compared in each patient (pre vs. post). Repeated-measures ANOVA were used to assess the main effects and the interaction [treatment (iTBS vs. i8Hz) ×

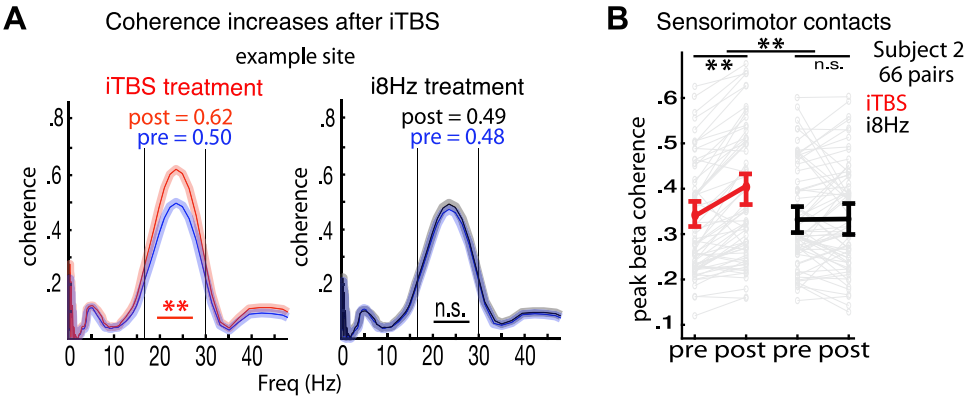

Figure 4. Intermittent θ-burst stimulation (iTBS) increases β coherence in sensorimotor cortex, whereas intermittent α-burst stimulation (i8Hz) does not. *A*: treatment effects for an example site located in the motor cortex of *patient 2*. β Coherence is enhanced after iTBS but not after i8Hz (red line pointwise significance level marked with **, α = 0.01; shaded areas indicate SE). *B*: averaged peak β coherence for all sensorimotor pair combinations before and after treatments (iTBS, red line; i8Hz, black line) in *patient 2* (66 pairs). Gray shade lines show the mean coherence peak for each single pair of contacts. Significant effects are marked with **, $P < 0.01$. n.s., Not significant.

time (pre vs. post), $P < 0.05$]. Post hoc analysis (paired nonparametric tests) evaluated differences between matched samples in iTBS and i8Hz (Wilcoxon signed-rank tests, $P < 0.01$) (Figs. 4*B* and 5). Similar statistical tests were used to compare the spectral power across treatments. The coherence in the intertrain analyses (Fig. 6*D*) was calculated similar to the coherence during the pre/posttreatment periods except that the analyses window was 6-s duration (+ 0.1 to 6.1 s after each 2-s train offset), sliding 500 ms at a time (1/6 = 0.16-Hz resolution). The peak coherence in the β band (12–30 Hz) was determined after each train (No. 1–20) for each contact pair, and a linear regression was fitted to the resultant values to compute the slope of the function for each electrode contact. Statistical difference between slopes across treatment conditions was evaluated using a two-way ANOVA and paired nonparametric tests (Wilcoxon signed-rank tests, $P < 0.01$) (Fig. 6*E*).

RESULTS

Treatment Sites

All seven patients selected for this study had ample electrode coverage of cortical sensorimotor areas (Fig. 5*A*). Selection of treatment sites was based on their function. For each patient, the electrode contact pair that elicited the most selective motor responses during HFSM was selected as a treatment site (Fig. 1*A*). Isolated (thumb and/or first) finger movements contralateral to the site of stimulation were elicited in five patients, whereas additional recruitment of

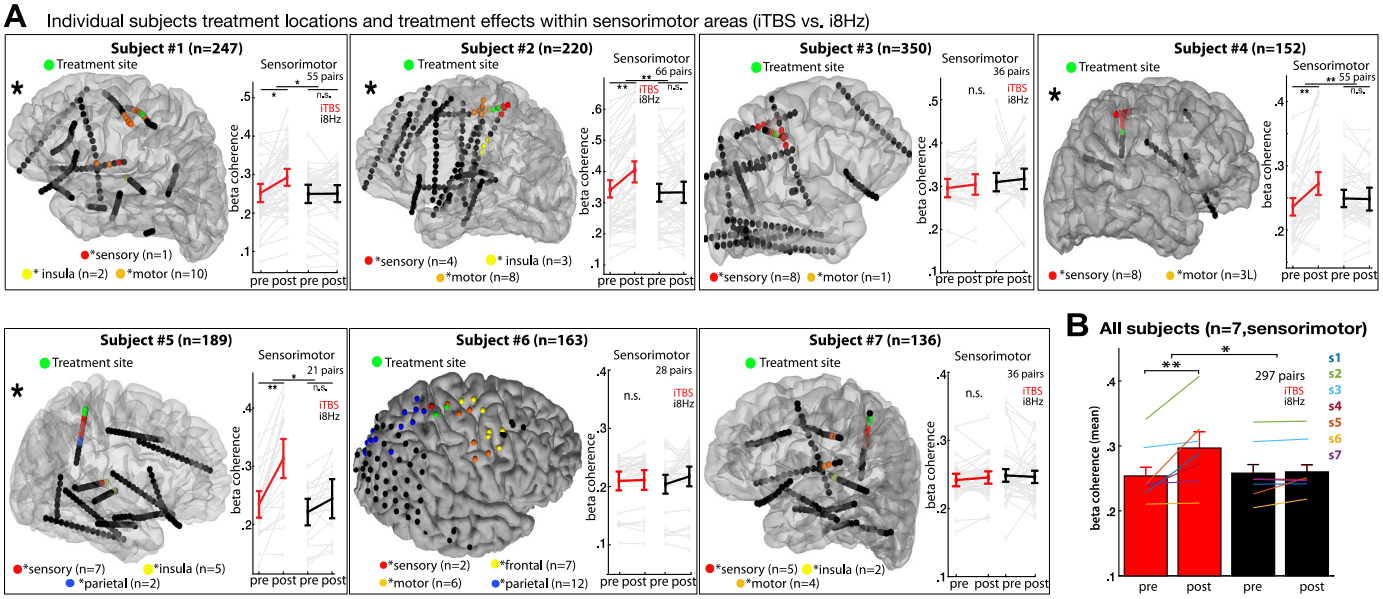

Figure 5. Intermittent θ-burst stimulation (iTBS) increases β coherence in the sensorimotor cortex across the population data. *A*: individual subjects MRI and electrode locations. Treatment sites (green dots). Read-out sites (colored dots) represent electrode contacts with significant corticocortical-evoked potentials (CCEPs) when stimulating the treatment site (contacts with effective connectivity to the treatment site). Most read-out contacts were close to the treatment site in the somatosensory (red) and motor (orange) cortices, but also more distally in the insula (*patients 1*, *2*, *5*, and *7*, yellow dots), parietal (*patients 5* and *6*, blue dots), and frontal (*patient 6*, yellow dots) cortices. *Inset*: individual subjects β coherence for all contact pairs in the sensorimotor cortex before and after treatments [thin gray lines show the coherence for each contact pair and thicker lines, the averaged coherence for iTBS (red) and i8Hz (black)]. iTBS increases β coherence in the sensorimotor cortex in 4/7 subjects. Significant effects are marked with asterisks. *B*: population data: averaged β coherence for all sensorimotor electrode contacts pairs across the 7 patients (297 pairs). Overlaid colored lines show the averaged β coherence for each patient individually. Significant effects are marked with * and ** ($P < 0.05$ and 0.01, respectively). i8Hz, intermittent α-burst stimulation; n.s., not significant.

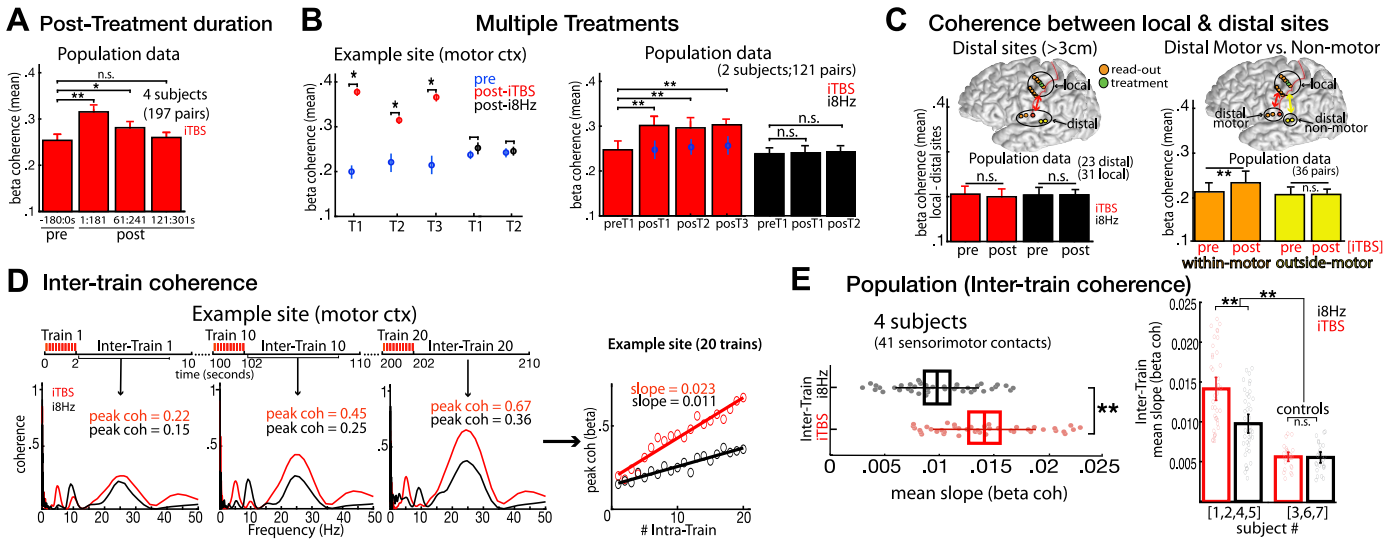

Figure 6. Intermittent θ-burst stimulation (iTBS) effects are frequency, spatially and temporally specific. *A*: posttreatment duration after-effects: iTBS induced increases in β coherence outlasted the duration of stimulation by 3 min—strongest effects occur during the initial 2 min (0–2 min), mild effects during 1–3 min, and washed 2–4 min after treatment offset. Significant effects are marked with asterisks. *B*: multiple treatments effects; *left*: sequential application of iTBS treatments up to 3 times (3 × 600 total pulses, 5-min gaps in-between) does not further increase β coherence for an example contact pair in the motor cortex (iTBS, red dots; pretreatment baseline, blue dots; i8Hz, black dots). *Right*: averaged data from all sensorimotor contact pairs in 2 patients (n = 121). Blue dots show the coherence values during the 2-min period before the corresponding treatment. *C*: coherence between local and distal sites. *Left*: example MRI brain from *patient 1*; white circle shows the 3-cm boundary around the treatment site. Contacts outside this boundary were considered distal (e.g., contacts in the insular, parietal, and most lateral and contralateral sensorimotor cortices). Bar plot shows the averaged β coherence between local and distal contacts (4 patients) which was not affected by either treatment. *Right*: MRI image depicts the coherence between focal and distal contacts that are still within sensorimotor cortices (orange arrow) vs. those distal contacts that are outside the sensorimotor cortex (yellow arrow). Bar plot shows the averaged β coherence for the population data (iTBS treatment only) between local and *1*) distal contacts within sensorimotor cortex (orange bars) and *2*) distal contacts outside sensorimotor cortex (yellow bars). Coherence within sensorimotor areas was larger (9 contacts within vs. 9 contacts outside the sensorimotor area; 36 contact pairs; note the equal length of the orange and yellow arrows showing that the distance between pairs was matched across groups). *D*: intertrain effects: buildup of coherence within a stimulation block for iTBS and i8Hz. *Left*: example contact pair within the motor cortex showing increases in β-coherence peak values from *trains 1*, *10*, and *20*. *Right*: linear function fitted to the β-coherence peaks from *trains 1–20* shows coherence increasing linearly with steeper slope in iTBS. *E*, *left*: mean slopes across the population data (*subjects 1*, *2*, *4*, and *5*; n = 41 sensorimotor contacts) are larger in iTBS compared with i8Hz. *Right*: averaged slopes across the population data for subjects with significantly increased post-iTBS β coherence and those without (*control subjects 3*, *6*, and *7*; n = 26 sensorimotor contacts). Significant effects are marked with * and ** (P < 0.05 and 0.01, respectively). coh, Coherence; ctx, cortex; i8Hz, intermittent α-burst stimulation; n.s., not significant; pre, pretreatment; preT1, pretreatment 1; postT1, posttreatment 1; T1, treatment 1.

wrist and biceps was elicited in two patients (Table 1). Contact pairs were in the primary motor cortex (both stimulating contacts anterior to the central sulcus, *patient 1*), in the primary somatosensory cortex (both contacts paracentral, immediately posterior to the central sulcus, *patients 5* and *7*), and in the sensorimotor cortex (1 contact immediately posterior to the central sulcus and the other anterior to it, *patients 2*, *3*, *4*, and *6*) (Fig. 1*A*). Seizure-onset foci was confirmed outside the sensorimotor areas in all patients (Table 1).

Read-Out Sites

After determining the treatment site in each patient, we chose read-out electrode contacts based on significant responses during CCEP mapping. From a total of 1,250 contacts recorded across 7 patients, 67 passed our selection criteria of exceeding a t statistic > 6 SD 10- to 50-ms poststimulation (35 in sensory/paracentral, 28 in motor, and 4 in premotor cortices, Figs. 1*A* and 4*A*). An additional 26 contacts also exhibited significant CCEPs but were outside the sensorimotor regions. Figure 3*A* shows the results for an example subject. Single-pulse stimulation applied to the treatment site (electrode array *A1*, *contacts 7–8*, located in the medial motor cortex) elicited significant CCEPs not only in contacts near to the stimulation site (*A1 contacts 5–10* and *A2 contacts 7–12*) but also in more distant contacts (*A3* with the deepest contacts located in the insula and another array with contacts located in the most lateral aspect of the sensorimotor cortex). One of our outcome measures was treatment-related changes in β coherence because β oscillations are the dominant spontaneously occurring network activity in the sensorimotor system (53, 54). Figure 3 illustrates that sensorimotor contact activities in our patients exhibited prominent β peaks during resting state before treatment. The averaged power spectra for two example contacts that were functionally connected to the treatment site within motor areas is shown in Fig. 3*B*. These contacts exhibited prominent spectral and coherence peaks at the β frequency (12–30 Hz). The dominant spectral power peaks and coherence peaks for the population of sensorimotor sites across the seven patients is shown in Fig. 3*C*. Spectral frequency peaks in power and coherence at other frequencies were also present in some sites together with the β peaks.

Treatment Effects of iTBS versus i8Hz Stimulation

Figure 4*A* shows an example electrode contact pair from the 12 read-out sensorimotor contacts selected (based on CCEP mapping) in one example subject. This contact pair

shows increased β coherence after iTBS treatment compared with before treatment (Wilcoxon signed-rank test, $P < 0.01$). β Coherence after i8Hz did not significantly change (Wilcoxon signed-rank test, $P = 0.29$). Figure 4*B* shows the β-coherence results across all contacts pairs in this patient ($n = 66$ pairs combinations from 12 contacts showing significant CCEPs to the stimulation site). There was a significant interaction between treatment (iTBS vs. i8Hz) and time (pre- vs. posttreatment) [repeated-measures (RM)-ANOVA, $F = 6.1$, $P = 0.0012$], which was driven by an increased coherence in the β band after iTBS compared with before (Wilcoxon signed-rank test, $P < 0.001$).

Figure 5 shows the results across the population data for the seven patients. From a total of 93 contacts with significant connectivity (based on CCEP mapping), we selected 67 contacts located in the sensorimotor cortex (39 contacts posterior to the central sulcus and 28 anterior to it) for our analyses of coherence (297 contact pairs combinations total). iTBS increased β coherence in the sensorimotor cortex in four out of seven patients, whereas i8Hz did not increase β coherence in any of the patients. A repeated-measures ANOVA with treatment (iTBS vs. i8Hz) and time (pre- vs. posttreatment) across contacts (67 contacts with significant CCEPs located within the sensorimotor cortex across all 7 patients) showed a significant interaction ($F = 6.34$, $P = 0.025$). This result was driven by an increased coherence in the β band after iTBS compared with before (Wilcoxon signed-rank test, $P = 0.002$). β Coherence before and after the i8Hz treatment did not differ significantly at the population level (Wilcoxon signed-rank test, $P > 0.1$, all patients) nor for any of the patients individually. The effect of iTBS was significant at the group level but individually only *subjects 1*, *2*, *4*, and *5* showed significant effects, whereas in *subjects 3*, *6*, and *7*, the effect did not reach significance (Wilcoxon signed-rank test, both $P > 0.1$). This raises the question whether β coherence changes more in subjects with stronger prestimulation β coherence within the sensorimotor network.

Treatment effect is frequency specific.

The iTBS-induced effects were specific to the β-frequency band (Fig. 5). Across all subjects, no treatment effect was found in the frequency bands α (8–12 Hz), low γ (60–80 Hz), high γ (80–150 Hz), and θ (4–7 Hz) (both $P > 0.4$; data not shown). However, varying effects were found in the θ and α bands in individual patients. For example, iTBS treatment increased θ coherence in *patients 2* and *3* (Wilcoxon signed-rank test, both $P < 0.05$), it reduced α coherence in *patient 6* (Wilcoxon signed-rank test, $P = 0.003$), whereas no significant changes were observed in the other four (both θ and α bands, $P > 0.4$). The i8Hz treatment increased coherence in the α band (8–12 Hz) in one patient (Wilcoxon signed-rank test, $P = 0.002$), whereas no significant changes were observed in the other six (Wilcoxon signed-rank test, both $P > 0.2$).

Treatment effect lasts ~3 min.

The increase in β coherence was the strongest immediately after the entire block of iTBS treatment (+1:181 s posttreatment compared with −180:0 s pretreatment, Wilcoxon signed-rank test, $P < 0.001$) (Fig. 5*A*). The increased coherence effect was still significant but weaker during the 1- to 3-min posttreatment period (+61:241 s, pre vs. post, Wilcoxon signed-rank test, $P = 0.015$), and it washed out for the 2- to 4-min posttreatment period (+121:301 s, pre vs. post, Wilcoxon signed-rank test, $P = 0.18$).

Multiple treatments do not result in further coherence increments.

Next, we tested in two subjects whether repeated application of iTBS treatments resulted in gradual increments in β coherence. Figure 6*B* shows the effects of three consecutive iTBS treatments (3 × 600 pulses separated by a 5-min intertreatment interval) for a pair of contacts in the motor cortex (left) and across the population data (right, 2 subjects, 121 contact pairs within sensorimotor networks). The increase in β coherence after the first iTBS treatment was very similar compared with the second and third treatments (pre vs. post, Wilcoxon signed-rank test, both $P < 0.001$). To avoid potential residual treatment effects, we used the 2-min period preceding the first treatment as the "pre" baseline period (preT1) for all comparisons in this analysis, and the 2 min after each treatment (postT1, postT2, and postT3), as the "post" period. The possibility of a ceiling effect after the first treatment was ruled out, as comparisons of the β coherence between the 2-min periods preceding each treatment (preT1 vs. preT2 vs. preT3, blue dots) revealed no significant differences (Wilcoxon signed-rank test, all $P > 0.31$). This result suggests that β-coherence values had mostly recovered to baseline levels before the onset of *treatments 2* and *3*. Multiple i8Hz treatments did not significantly change β coherence (pre vs. post, Wilcoxon signed-rank test, both $P > 0.2$).

Treatment effect is specific to sensorimotor areas.

We quantified whether the enhanced β coherence after iTBS treatment observed in *patients 1*, *2*, *4*, and *5* was limited to read-out contacts near the treatment site (e.g., connected contacts within sensorimotor cortices <3 cm from the treatment site) or extended to other, more distant yet connected (based on CCEP mapping) regions such as the insula (Fig. 6*C*, *left*). Distal contacts were in the insular (55), parietal (53), and more lateral aspects of the motor (56) and somatosensory (52) cortices and were averaged across areas and subjects before statistical testing (all 4 subjects had distal contacts including No. 4 in the opposite hemisphere; Fig. 5*A*). β Coherence between focal ($n = 31$) and more distant contacts ($n = 23$) was not significantly changed after either treatment (RM-ANOVA, stimulation × time interaction, $F = 0.6$, $P = 0.41$; pre vs. post, Wilcoxon signed-rank test, both treatments $P > 0.1$). These results suggest that iTBS-enhancement effects are relatively local within sensorimotor regions (<3 cm from the treatment site). To examine the focal versus network specificity of the iTBS-enhancement effect, we selected contacts within sensorimotor areas and compared them with other equally distant contacts that were outside sensorimotor areas. Contacts within sensorimotor areas located in the more lateral aspect of the sensorimotor cortices (>3 cm away from the treatment site, 9/67) showed enhanced β coherence compared with other equally distant contacts outside sensorimotor areas (Fig. 6*C*, *right*; distal sensorimotor contacts, pre-iTBS vs. post-iTBS, Wilcoxon signed-rank test, $P = 0.019$; distal nonsensorimotor

contacts, pre-iTBS vs. post-iTBS, Wilcoxon signed-rank test, P = 0.36). This result suggests a network-specific iTBS-enhancement effect rather than just a focality effect.

Treatment effect builds up linearly.

To determine the time course of the treatment effect during the stimulation block (e.g., intertrain), we quantified the effect of each single-stimulation train (from *train 1* to *20*) (Fig. 6*D*). Coherence between sensorimotor contacts was calculated in the 20 consecutive intertrain intervals during the two treatment types (8 s for iTBS, 10 s for i8Hz). The analysis window was set similar for both treatments from +0.1 to 6.1 s after each train offset, as the effects were stronger within this time interval. Figure 6*D* shows increased β-coherence values as a function of increasing intertrain trial for a sample electrode pair. Intertrain β-coherence values increased more strongly during iTBS compared with i8Hz treatment. The β-coherence peaks during iTBS increased steadily from 0.22 (*train 1*) to 0.67 (*train 20*), whereas a weaker effect occurred during i8Hz (from 0.15 in *train 1* to 0.36 in *train 20*). We quantified the effect by fitting a linear regression line to the 20 coherence peak values and calculating the slope of the fitted function for each electrode contact. Steeper slopes indicate larger increases in coherence values (slope iTBS = 0.0243 vs. slope i8Hz = 0.011). Across the population data (4 subjects), slopes derived from within iTBS intertrains were steeper compared with those from i8Hz (Wilcoxon signed-rank test, P = 0.011) (Fig. 6*E*, *left*). Only contacts within the sensorimotor cortex in subjects that showed significant posttreatment effects after iTBS were included in this analysis (*subjects 1*, *2*, *4*, and *5*, 41 contacts). A comparison between these subjects and those that showed no significant posttreatment effects (*subjects 3*, *6*, and *7*, 26 contacts) revealed that the latter group also displayed flatter slopes during the treatment (Fig. 6*E*, *right*). A two-way ANOVA, with factors of group (posttreatment-sensitive vs. posttreatment-insensitive) and intertrain (iTBS vs. i8Hz), showed significant effects of group (F = 174.5, P = 0.0016), intertrain (F = 20.81, P = 0.00018), and group × intertrain interaction (F = 19.49, P = 0.0002). The interaction effect was driven by increased slopes during iTBS treatment in the posttreatment-sensitive group (Wilcoxon signed-rank test, $P < 0.0001$).

Previous studies (21, 57) found treatment effects on CCEP amplitude (pre vs. post). We tested this hypothesis by applying single pulses at ~1 Hz (300-ms jitter, ~200 pulses) before and after the resting periods preceding and following treatment, but no treatment effects were found on the P1 amplitude of CCEPs across the population data (Wilcoxon signed-rank test, both iTBS and i8Hz, $P > 0.2$).

Individual differences between treatment responders and nonresponders.

Some subjects (4/7) showed significant treatment effects (enhanced β coherence after iTBS and gradual buildup during iTBS), whereas others did not. Here, we test for additional factors that could potentially account for the differences between responders and nonresponders.

Specific location of the stimulation site. To determine whether the difference between responders and nonresponders was related to the specific placement of the stimulation electrodes within the sensorimotor cortex, we divided the subjects in three groups (M1 motor vs. S1 sensory vs. M1 + S1 sensorimotor) depending on where the stimulation was applied to (Fig. 7*A*). The M1 group contains 55 contact pairs (all from *subject 1*), the S1 group contains 59 pairs (from *subjects 5* and *7*), and the M1 + S1 group contains 175 pairs (from *subjects 2*, *3*, *4*, and *6*). Figure 7*B* shows the averaged β coherence in the three locations. Treatment effects were significant in all three locations (Wilcoxon signed-rank test, all $P < 0.011$), suggesting that the observed differences between responders and nonresponders could not be explained based on anatomical variability in the treatment sites (Fig. 7*B*).

Distance between the treatment and read-out sites. To determine whether the difference between responders and nonresponders was related to the distance between the treatment and read-out electrode contacts, we compared the distance between them in the two groups of subjects separately. Figure 7*C* shows no significant differences between the two groups [Mann–Whitney U test, P = 0.473; responders, mean = 23.5 mm, 95% CIs = (10.3–26.1); nonresponders, mean = 20.1 mm, 95% CIs = (10.8–20.6)]. This means that, in average, read-out contacts were as far apart from the stimulation sites in responders and nonresponders and suggests that this factor could not account for the effects.

Distance between read-out sites. Given that treatment effects reflect changes in coherence between read-out contacts, it is possible that the difference between responders and nonresponders was related to the physical distance between read-out contact pairs. Figure 7*D* shows no significant differences between the two groups [Mann–Whitney U test, P = 0.292; responders, mean = 26.10, 95% CIs = (4.04–63.55); nonresponders, mean= 23.89, 95% CIs = (4.24–53.94)]. This means that, in average, read-out contacts were as far apart from each other in responders and nonresponders and suggests that this factor could not account for the effects. Moreover, overall baseline coherence values (before treatment) scaled down with increasing distance between read-out contacts very similarly in both, responders and nonresponders (Fig. 7*E*). A linear regression was fitted to each group data and very similar parameters were observed (responders: slope = −0.0037, Pearson's correlation coefficient = −0.7153, $P < 0.001$; nonresponders: slope = −0.0034, Pearson's correlation coefficient = −0.8224, $P < 0.001$).

Preexistent spectral properties. To determine whether the difference between responders and nonresponders was related to preexistent spectral properties within the sensorimotor network, we compared the coherence before treatment at different frequency bands between the two groups. Figure 8*A* shows that pretreatment coherence values in the β band did not differ between responders and nonresponders (Mann–Whitney U test, Z = −0.84, P = 0.401). As for the α-frequency band, although overall coherence values in this band were smaller than those in the β band (mean α coherence = 0.13; mean β coherence = 0.26), nonresponders showed significantly larger α-coherence values than responders (Mann–Whitney U test, Z = −7.62, $P < 0.001$) (Fig. 8*B*). Other frequency bands showed no significant differences between subjects' groups (δ, θ, γ low, γ high, Mann–Whitney U test, all $P > 0.2$, data not shown). Next, we tested whether pretreatment coherence in the α band could predict treatment

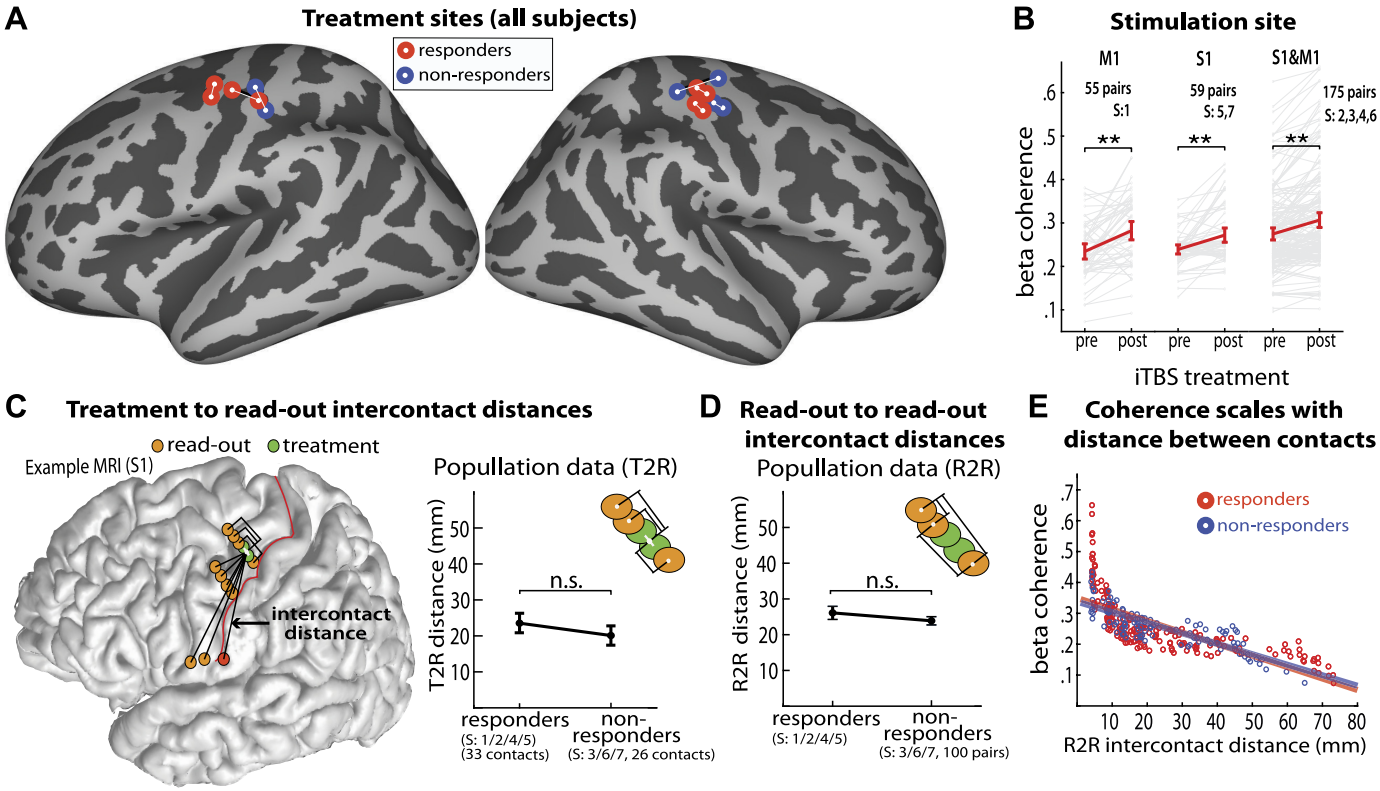

Figure 7. Treatment effects do not depend on the specific stimulation site location within sensorimotor cortex nor on the physical distance between sites. *A*: electrode contacts used for stimulation in all 7 patients registered onto a common brain surface (lines in-between contacts represent bipolar stimulation). Contacts in patients with significant treatment effects (responsive, red dots) and null effects (nonresponsive, blue dots). Red and blue sites are intermixed. *B*: treatment effects separated according to the location of the stimulation site: motor (M1) vs. sensory (S1) vs. sensorimotor (M1 + S1). Treatment effects were significant for all site locations. Error bars indicate ±1 SE. *C*: intercontact distances between treatment sites (middle point between anode and cathode) and read-out contacts (central point) in responders vs. nonresponders. *D*: intercontact distances between read-out contacts in responders vs. nonresponders. *E*: coherence values pre-iTBS treatment decrease with increasing distance between read-out contacts in both responders and nonresponders. Significant effects are marked with ** ($P < 0.01$). Red dots, responders (197 pairs). Blue dots, nonresponders (100 pairs). Color lines, linear regression data fit. iTBS, intermittent θ-burst stimulation; n.s., not significant.

efficacy in the β band (Fig. 8*C*). This was done by calculating a treatment gain index in the β band [(post-iTBS − pre-iTBS)/(post-iTBS + pre-iTBS)] and correlating it against the pretreatment α-coherence values for each contact pair and subject group. There was a small but significant negative correlation between these two factors with treatment gains being inversely correlated to pretreatment α-coherence values in both responders and nonresponders (responders, Pearson's correlation coefficient = −0.38, $P < 0.001$; nonresponders, Pearson's correlation coefficient = −0.27, $P < 0.001$). Coherence values in the α band were more variable across sites in nonresponders compared with responders (nonresponders, CV = 0.46; responders, CV = 0.26). As expected, treatment gains were larger in responders [responders, mean = 10.04, 95% CI = (−10.37, +35.87); nonresponders, mean = 0.87, 95% CI = (−8.56, +11.04); Mann–Whitney *U* test, $Z = 7.37$, $P < 0.001$].

Dynamic range of treatment effects. We tested whether the treatment gain at a given site was proportional to its preexistent β oscillatory amplitude (Fig. 8*D*). This was done by calculating a treatment gain index in the β band [(post-iTBS − pre-iTBS)/(post-iTBS + pre-iTBS)] and correlating it with the pretreatment β-coherence values for each contact pair and subject group. We found a negative correlation between these two factors in responders (Pearson's correlation coefficient = −0.25, $P < 0.001$). This result suggests a specific dynamic range where sites with preexistent β-coherence values below ~0.35 Hz were more effectively amplified by the treatment (e.g., avoiding ceiling effects). As shown in Fig. 8*A*, pretreatment β coherence was not significantly different between subject groups [responders, mean = 0.266, 95% CIs = (0.126, 0.523); nonresponders, mean = 0.252, 95% CIs = (0.134, 0.369)].

DISCUSSION

We characterized the physiological effects of direct cortical iTBS, a novel rTMS-patterned stimulation, applied intracranially in the human sensorimotor cortex of patients with surgical epilepsy implanted with electrodes for clinical reasons unrelated to this study. We found that iTBS enhanced β coherence within sensorimotor networks. This effect was stimulation-pattern specific, as stronger effects were found using iTBS while α-frequency stimulation did not increase β coherence. This effect was limited to local, functionally connected somatosensory and motor cortical regions that share similar spectral profiles (β oscillations), and it lasted 3 min after treatment offset. The effect occurred in four out of

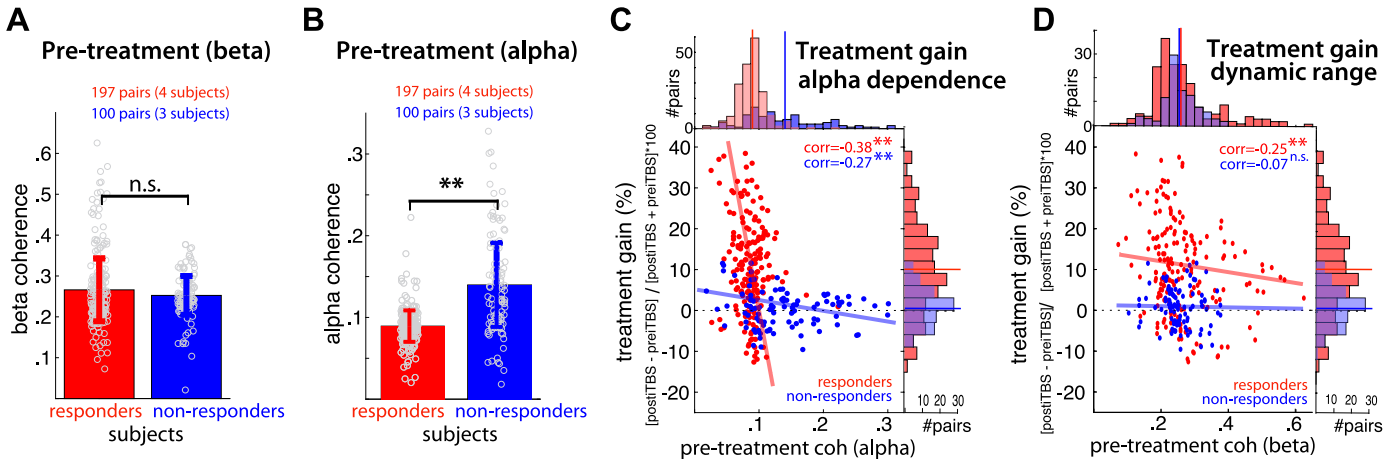

Figure 8. Treatment effects depend on preexistent α coherence and dynamic range of β oscillations. *A*: averaged β-coherence values in responders (red) and nonresponders (green) before treatment onset. Each gray dot represents a single site (197 contact pairs in responders and 100 in nonresponders). *B*: similar to *A* except that coherence values in the α-frequency band. *C*: treatment gain index in the β band [*y*-axis; (post-iTBS − pre-iTBS)/(post-iTBS + pre-iTBS) × 100)] against pretreatment α-coherence values (*x*-axis) for each contact pair and subject group. Red dots, responders (197 pairs). Blue dots, nonresponders (100 pairs). Color lines, linear regression data fit. Histograms are plotted over scatter plots for visualization of data distributions. Vertical lines, mean values for responders (red) and nonresponders (blue). *D*: same as *C* except that the *x*-axis represents pretreatment β-coherence values. Significant effects are marked with ** ($P < 0.01$). iTBS, intermittent θ-burst stimulation; n.s., not significant.

seven subjects and was predicted by a gradual increase in coherence during the course of the treatment itself. Other factors contributing to the interindividual differences were the baseline (preexistent) spectral profile within the sensorimotor network and the dynamic range of β-coherence amplitudes (ceiling effects). Our results provide a starting point for clinicians and researchers to design more optimal stimulation protocols aiming at inducing neuroplasticity in cortical networks using direct intracranial electrical stimulation.

Patterned Electrical Stimulation Advantages

The stimulation parameters used in this study were informed by rTMS studies aimed at inducing neuroplasticity effects (17–19, 58). The implementation of iTBS into rTMS paradigms has shortened rTMS treatment duration (40 min with conventional 10 Hz vs. 15 min with iTBS) while achieving similar or greater treatment effects (18, 59). Invasive approaches using epidural, cortical, and deep brain stimulation are increasingly used to treat movement/neuropsychiatric disorders and epilepsy (25, 60, 61) and investigated to assist motor recovery following strokes and traumatic brain injuries (1, 8, 62). Although the exact mechanisms underlying treatment effects using these invasive stimulation approaches are still largely unknown, neuroplastic changes are thought to play a significant role (13, 14, 63, 64). The goal of the present study is to determine the dynamics and spectral features of the potential neuroplastic changes that occur within the sensorimotor cortex during and after direct cortical iTBS (DCS-iTBS).

Direct Invasive Electrical Stimulation versus TMS

Our invasive protocol (DCS) shares similar stimulation parameters with noninvasive rTMS protocols (e.g., patterned repetitive TBS); however, frequency is not the only factor. The electrical field caused by direct electrical stimulation applied to the cortex (DCS) is thought to directly activate by and large the pyramidal cell fibers, that is, the largest and most excitable neurons in the cortex (65, 66). In contrast, rTMS delivers repetitive electric field pulses (E-field) through a coil placed over the scalp. This coil generates a magnetic field that efficiently passes through the skull, allowing magnetic pulses to induce strong and moderately spatially focal currents in the underlying brain tissue. Field modeling (67, 68) and concurrent TMS with neuroimaging [PET (69), fMRI (70), or EEG (71)] studies showed that TMS stimulates large neuronal populations en masse through the generation of not only indirect (I) waves (transynaptic spread) but also direct (D) waves (direct activation of neurons) (72, 73). Thus, the mechanisms of action between DCS and rTMS likely differ in important ways, although they have not yet been fully elucidated for either approach.

There is also a difference in the spatial extent of the stimulated area between the approaches. Although it is difficult to exactly estimate the spread of activation caused by the stimulation in our study, single-cell recordings in animals using much smaller electrodes (electrode tip: 5 × 10 μm) showed lateral spread of activation in the cortex between 1 and 4 mm from the electrode tip depending on current amplitude (66). Another estimate based on stereo EEG (sEEG) stimulation in the human occipital cortex, using similar sEEG electrodes as the ones used in our study (Fig. 1*B*) and a continuous bursting pattern of stimulation (not iTBS), found that the size of the affected cortical area was also in the millimeter radius range (74). The affected cortical volume in TMS in the short-latency activation volleys (TMS-evoked action potentials) ranges from a few cubic millimeters to centimeters, depending on several physical factors such as stimulation intensity and coil design (70, 75, 76). The focal spread of our treatment effects is supported by invasive studies that showed the majority of modulated regions being anatomically and functionally closer to the stimulation site (21, 34). Regarding the focal versus network specificity of the effect, electrode contacts that were within sensorimotor areas and near the

treatment site showed the strongest iTBS effects (Fig. 6*C*, *left*). However, contacts that were more distant from each other yet within sensorimotor areas (medial vs. lateral portions of the motor cortex) also showed increased β coherence compared with other equally distant contacts that were outside sensorimotor areas (e.g., insula) (Fig. 6*C*, *right*). This result suggests a network-specific effect rather than just a focality effect.

The goal of the present study, however, was not to equate these different methods of stimulation but to test whether the most effective parameters in TMS (e.g., rTMS-iTBS) can also induce neuroplastic changes when applied intracranially with a different stimulation technique. Further studies using rTMS in patients with concurrently implanted recording (iEEG and chronic) and stimulating (DBS and DCS) electrodes are needed to more directly compare these methods. The safety of such protocols is under active investigation (77, 78) with some evidence suggesting that TMS does not deliver damaging stimuli in patients with DBS with reported voltages up to 0.7 V induced between pair of contacts (79).

Spatial and Spectral Specificity of iTBS Treatment Effects

A key result from our work is that iTBS treatment increased coherence specifically within the sensorimotor system and at β (12–30 Hz) frequencies. Importantly, areas within the sensorimotor cortices already exhibited prominent coherence peaks in the β band before treatment (Fig. 3, *B* and *C*), suggesting that iTBS enhanced connectivity of already preexistent rhythms. Prior studies showed that the frequency of stimulation is an important factor in driving specific clinical outcomes in patients with Parkinson's disease (PD) (11, 42, 80, 81), in patients with epilepsy (15, 60), in modulating focal excitability in macaque brains (57), and in prolonging the duration of the effects (acute vs. plasticity) (61, 82, 83). An important question is "Why θ- and not α-frequency stimulation affected β coherence?" α is a harmonic of β, and α-frequency oscillations are more strongly represented in sensorimotor areas compared with θ, suggesting that α stimulation could have more likely affected β coherence. It is possible that patterned stimulation with θ bursts mimics the natural patterns of brain activity in sensorimotor cortex more accurately than i8Hz (repetitive single pulses delivered at 8 Hz). Thus, iTBS could increase synaptic strength between the stimulated neurons and interconnected ones, which increases resonance at the most prominent frequency within these sensorimotor networks. More-over, although the iTBS-enhancement effect was frequency specific, it was not directly proportional to the magnitude of β-rhythm prestimulation, as subjects that showed the enhancement effect after iTBS did not have stronger prestimulation β coherence compared with those that did not. This suggests that θ-burst stimulation does not increase preexistent rhythms directly proportional to their presence and that other factors inherent to sensorimotor network dynamics might contribute.

One such factor is the presence of preexistent rhythms in other, potentially competing, frequency bands. Although overall coherence values in the α band were smaller in amplitude than the β band, we found that nonresponders showed higher pretreatment α coherence than the responders. Interestingly, the amount of α-coherence pretreatment was inversely correlated with the treatment gain in the β band. This result is in line with recent studies that recorded invasively from the sensorimotor cortex and observed that α- and β-band rhythms differed in their anatomical and functional properties (84, 85). In line with those studies, the increase in α-band coherence that we observed in nonresponders could be associated with differences in arousal state. In addition, we found that the strongest treatment gains (iTBS-related increases in β coherence compared with baseline) were not proportional to the strength of preexistent β oscillations in a given area. Sites with coherence values between 0.2 and 0.4 showed the strongest treatment effects. This result suggests a ceiling effect whereby the coherence between specific sites within the sensorimotor network could not be enhanced much more, a factor that should be considered in the design of effective treatment therapies.

Duration of Treatment Effects

Our cortical iTBS treatment effects outlasted the period of stimulation as β coherence remained elevated for ~3 min after treatment offset. Studies in mice hippocampus have convincingly shown long-lasting synaptic potentiation (LTP) effects outlasting iTBS for several hours and even days. However, iTBS treatments in animal models are delivered multiple times during hours, repeated over several days, and at high-amplitude currents. Evidence of iTBS-induced plasticity effects in human TMS studies are traditionally based on long-term excitability changes, as measured by MEP facilitation, which generally lasts up to 60 min after stimulation (18). Our increased β-coherence effects lasted only 3 min, a time window where usually MEPs are not facilitated yet (18). No EMG activity was recorded in our study, and thus, we cannot verify whether MEP facilitation was associated with β-coherence increase. MEP amplitude is considered the "gold-standard" measure and its facilitation after stimulation may truly reflect plasticity effects, whereas β coherence increase during/immediately after iTBS may reflect a mechanism underlying plasticity induction. In addition, intracranial iTBS effects are much more focal compared with TMS which stimulates large populations of neurons en masse (see *Direct Invasive Electrical Stimulation versus TMS*). In TMS, large charges are often applied at ≥100% the active motor threshold, which evoke descending waves of corticospinal activity and during longer periods of time (35 min), whereas our currents were applied at 80% motor threshold and for shorter time periods. And finally, unlike in the study by Keller et al. (21), we did not observe significant effects on CCEPs but on spontaneous β coherence during resting state. In summary, these points may indicate that β coherence is a highly sensitive measure of subtle yet important treatment-related changes particularly in intracranial stimulation procedures. Follow-up studies are needed to correlate these changes in β coherence to MEP and clinical measures.

Repeated-Treatment Effects

Recent human rTMS studies suggested that a single iTBS therapy session is insufficient to induce robust plasticity effects and that multiple sessions might provide benefit (27, 28). Our findings indicate that up to three intracranial iTBS treatments do not result in linear increases in β coherence in

line with a recent rTMS study (23), suggesting more complex dynamics that likely are subject and activity dependent (86). Future intracranial iTBS studies might confirm the number of sessions required to induce longer lasting effects in the human cortex. Analysis of activity within a single-treatment session (intertrain stimulation intervals) might clarify the time course of the treatment effects (34). Our results show that iTBS-mediated β-coherence effects scale more or less linearly with consecutive trains of stimulation and that this gradually developing effect correlates with the longer lasting changes in β coherence after the stimulation ends.

Treatment Types: iTBS versus α-Frequency Stimulation

Prior studies translating rTMS paradigms to intraparenchymal stimulation showed varying or weak results (21, 22), or did not report neurophysiological changes (42). For example, Keller et al. (21) stimulated several different brain regions across patients and found mixed excitation at some treatment locations and inhibition at others. The authors found that intermittent α-frequency stimulation of the dorsolateral prefrontal cortex (DLPFC) produced excitation in two subjects and suppression in the other two, whereas stimulation of temporal (1 subject) and motor (3 subjects) cortical regions produced suppression. In our study, we limited the treatment (and read-out) sites to one well-defined functional network (sensorimotor) and measured changes in excitability after trains of θ bursts (iTBS). Our results indicate that iTBS can enhance neuronal plasticity more effectively compared with α-frequency stimulation (i8Hz). As previously mentioned, another interesting result from our study was that, unlike Keller et al., we did not find significant effects on CCEPs but on spontaneous β coherence during resting state, indicating that this measure may be more highly sensitive to treatment-related changes. Another difference was that we did not observe significant effects on CCEPs in the motor cortex after trains of i8Hz stimulation. One possible explanation for this may be that CCEP stimulation was not applied immediately before and after the i8Hz stimulation because we were interested in recording coherence of resting networks without affecting it by any kind of stimulation pulse. The last CCEP pulse occurred at least 15 min before i8Hz stimulation onset, and the first CCEP pulse occurred at least 5 min after i8Hz stimulation offset (the same applies for iTBS). Moreover, our stimulation currents were applied at lower amplitudes (80% of the active motor threshold vs. 100%) and for shorter periods of time.

Treatment Efficacy beyond Sensorimotor Cortex

Since we characterized the physiological effects of cortical iTBS in the human sensorimotor cortex, the obvious question is about the generalizability of the results. A recent DBS study in patients with PD applied subcortical iTBS to the globus pallidus internus (GPi) and the subthalamic nucleus (STN) while recording from the DLPFC (22). They found that GPi stimulation (but not STN) modulated θ power in DLPFC, suggesting that iTBS can be effectively applied to other brain areas and cause frequency-specific effects (see also Ref. 87). In iTBS, trains of high-frequency (50 Hz) pulses are delivered at 5 Hz, which raises the question as to why a resonance frequency of ~5 Hz amplifies coherence in the β range in our results. β-Band oscillations are a dominant feature in the sensorimotor cortex (88), which includes movement-related β desynchronization (MRBD) during the preparation and execution of movement and postmovement β synchronization (PMBS) on movement cessation (53). Our iTBS treatments were applied during resting state while patients were quietly relaxed and β synchronization was presumably enhanced relative to the movement phase. One possibility is that iTBS further increases β synchronization and the resonance at the most prominent frequency within sensorimotor networks. Further research will need to confirm whether iTBS can amplify preexistent rhythms in specific brain areas or predominantly θ rhythms (87) or whether alternative approaches using close-loop stimulation (57, 89) and/or adaptive DBS (11) will be more efficacious.

Future Considerations and Pitfalls

Our iTBS treatments were applied during resting state, and no behavioral output was measured. Future studies might investigate whether intracranial sensorimotor cortex iTBS influences motor thresholds (MT) or MEP amplitudes and whether it can improve the execution and learning of specific motor tasks. In addition, measuring treatment effects during an active task (e.g., dynamic motor output task; 90) can also minimize state fluctuations that are important to reduce interindividual variability. Two DBS human studies applied TBS in the entorhinal white matter and found improvements in memory for portraits, whereas stimulation of the adjacent entorhinal gray matter of the subiculum did not improve memory (26, 91). Most of our patients (6/7) were implanted with sEEG arrays, and stimulation was applied through two contacts in a bipolar fashion spanning a total distance of 10 mm (Fig. 1*B*), which likely stimulated passing-by white matter tracts, contributing to the treatment effect (15). In fact, some of the contacts used for treatment were in the white-gray matter junction of the sensorimotor cortex. This might explain the null effect observed in *patient 6*, who was implanted with ECoG grids, as subdural stimulation spreading along the cortical convexity might less effectively excite white matter tracts compared with sEEG stimulation. This explanation cannot account for *subjects 3* and *7* who were implanted with sEEG and showed no significant treatment effects.

We did not find any systematic difference regarding the specific treatment locations, proximity to white matter tissue, intercontact distance between read-out contacts, or distance between treatment and read-out contacts. Further work comparing DBS programming strategies in bigger data sets (92) and electrical field modeling (56, 93) is needed to improve the interpretability of the results and reduce the wide interindividual differences regarding the ideal stimulation site relative to the cortex. Although our selection criterion was based on the clinical stimulation mapping results, others have selected their stimulation sites based on particular spectral features (87) or other criteria (11, 42). Thus, a consensus between scientist as to which criteria to use in the selection of treatment sites, as well as read-out sites, would be desirable.

A potential pitfall of this study is that it was conducted in patients with epilepsy that were taking antiepileptic drugs (AEDs) (Table 1). Several AEDs are known to modify cortical excitability and plasticity (94). For example, anticonvulsants

that block voltage-gated Na^+ channels such as carbamazepine can increase motor thresholds (94, 95). Only one of our patients (*patient 5*) was taking carbamazepine at the time of the experiment and he was a responder, suggesting that partial blockade of these Na^+ channels did not affect the iTBS-induced effects on this patient. Future studies will have to establish if the results generalize to other patient populations. To increase potential generalizability and due to safety precautions, we only included patients with their epileptogenic focus outside of the sensorimotor system and at least one gyrus removed from the treatment site (Table 1).

Conclusions

The therapeutic potential of rTMS-patterned stimulation paradigms using iTBS has proven to be a useful addition to the field of electronic medicine (18). Improved treatment efficacy of iTBS compared with conventional rTMS was shown in a variety of neurological disorders including stroke, PD, epilepsy, depression, obsessive compulsive disorder (OCD), and PTSD. Despite these promising results, a clear understanding of the underlying neurophysiological mechanisms in humans is lagging behind that observed in animal models where iTBS induces robust long-lasting effects on glutamatergic synapses. We bridge this gap by applying iTBS directly into the cortex of patients implanted with depth electrodes for reasons unrelated to the present study (epilepsy monitoring). We found that cortical iTBS induces stronger effects compared with α-frequency stimulation and that these effects are frequency and spatially specific. Specifically, iTBS applied to well-defined regions of the sensorimotor cortex at low-amplitude currents increases preexistent local synchrony in the β range. In summary, iTBS can enhance neuronal plasticity more effectively compared with other treatment modalities within a single experimental session. Our results indicate that iTBS enhancement is frequency dependent, it occurs within local sensorimotor networks that share similar spectrotemporal properties (β oscillations) and relies on the development of neuronal synchrony during the course of the iTBS treatment itself. Our findings might help explain part of the heterogeneity in the results across studies using repetitive stimulation and strongly suggests that standard iTBS protocols (either noninvasive or invasive) consider the individuals excitability profile particularly preexistent rhythms in a given cortical area and their sensitivity to gradual changes in synchrony during the course of the treatment.

ACKNOWLEDGMENTS

We are indebted to all patients who volunteered their time to participate in our study. We also thank the staff of the Epilepsy Monitoring Unit at North Shore University and Lenox Hill Hospitals for support throughout the conduction of the studies. We thank Nima Mesgarani and Stavros Zanos for providing helpful feedback on the manuscript. We thank Tucker Davis Technologies (Mark Hanus and Myles Billard) for support with the neural recording and stimulation equipment.

GRANTS

This work was supported by the National Institutes of Health (Grant Numbers R01MH111439, U01NS098976, and P50MH109429 to A.M., S.B., and J.L.H.), New York States Empire Clinical Research Investigator Program (ECRIP) Fellowship (to A.M. and S.B.), and the Mind & Life Institute Varela Award (Grant Number A-30161710 to J.L.H.).

DISCLOSURES

No conflicts of interest, financial or otherwise, are declared by the authors.

AUTHOR CONTRIBUTIONS

J.L.H. and A.D.M. conceived and designed research; J.L.H. and A.S. performed experiments; J.L.H. and A.M. analyzed data; J.L.H., A.D.M., and S.B. interpreted results of experiments; J.L.H. and N.M. prepared figures; J.L.H. drafted manuscript; J.L.H., A.S., A.D.M., and S.B. edited and revised manuscript; J.L.H., A.S., A.M., N.M., A.D.M., and S.B. approved final version of manuscript.

REFERENCES

1. **Marquez-Chin C**, **Popovic MR.** Functional electrical stimulation therapy for restoration of motor function after spinal cord injury and stroke: a review. *Biomed Eng Online* 19: 34, 2020. doi:10.1186/s12938-020-00773-4.
2. **Davis P**, **Gaitanis J.** Neuromodulation for the treatment of epilepsy: a review of current approaches and future directions. *Clin Ther* 42: 1140–1154, 2020. doi:10.1016/j.clinthera.2020.05.017.
3. **Tsuboyama M**, **Lee Kaye H**, **Rotenberg A.** Biomarkers obtained by transcranial magnetic stimulation of the motor cortex in epilepsy. *Front Integr Neurosci* 13: 57, 2019. doi:10.3389/fnint.2019.00057.
4. **Sigurdsson HP**, **Jackson SR**, **Kim S**, **Dyke K**, **Jackson GM.** A feasibility study for somatomotor cortical mapping in Tourette syndrome using neuronavigated transcranial magnetic stimulation. *Cortex* 129: 175–187, 2020. doi:10.1016/j.cortex.2020.04.014.
5. **Daskalakis ZJ**, **Dimitrova J**, **McClintock SM**, **Sun Y**, **Voineskos D**, **Rajji TK**, **Goldbloom DS**, **Wong AHC**, **Knyahnytska Y**, **Mulsant BH**, **Downar J**, **Fitzgerald PB**, **Blumberger DM.** Magnetic seizure therapy (MST) for major depressive disorder. *Neuropsychopharmacology* 45: 276–282, 2020. doi:10.1038/s41386-019-0515-4.
6. **Perera T**, **George MS**, **Grammer G**, **Janicak PG**, **Pascual-Leone A**, **Wirecki TS.** The clinical TMS society consensus review and treatment recommendations for TMS therapy for major depressive disorder. *Brain Stimul* 9: 336–346, 2016. doi:10.1016/j.brs.2016.03.010.
7. **Polosan M**, **Leentjens AFG.** Deep brain stimulation in obsessive-compulsive disorder. In: *Fundamentals and Clinics of Deep Brain Stimulation: an Interdisciplinary Approach*, edited by Temel Y, Leentjens AFG, de Bie RMA, Chabardes S, Fasano A. Cham, Switzerland: Springer International Publishing, 2020, p. 263–278.
8. **Ovadia-Caro S**, **Khalil AA**, **Sehm B**, **Villringer A**, **Nikulin VV**, **Nazarova M.** Predicting the response to non-invasive brain stimulation in stroke. *Front Neurol* 10: 302, 2019. doi:10.3389/fneur.2019.00302.
9. **Philip NS**, **Barredo J**, **Aiken E**, **Larson V**, **Jones RN**, **Shea MT**, **Greenberg BD**, **van 't Wout-Frank M.** Theta-burst transcranial magnetic stimulation for posttraumatic stress disorder. *Am J Psychiatry* 176: 939–948, 2019. doi:10.1176/appi.ajp.2019.18101160.
10. **Ramirez-Zamora A.** Acute neuropsychiatric symptoms and impulse control disorders after subthalamic nucleus deep brain stimulation. In: *Deep Brain Stimulation: A Case-based Approach*, edited by Chitnis S, Khemani P, Okun MS. New York: Oxford University Press, 2020, p. 149–154.
11. **Ramirez-Zamora A**, **Giordano J**, **Gunduz A**, **Alcantara J**, **Cagle JN**, **Cernera S**, **Difuntorum P**, et al. Proceedings of the Seventh Annual Deep Brain Stimulation Think Tank: advances in neurophysiology, adaptive DBS, virtual reality, neuroethics and technology. *Front Hum Neurosci* 14: 54, 2020. doi:10.3389/fnhum.2020.00054.
12. **Puig-Parnau I**, **Garcia-Brito S**, **Faghihi N**, **Gubern C**, **Aldavert-Vera L**, **Segura-Torres P**, **Huguet G**, **Kádár E.** Intracranial self-stimulation modulates levels of SIRT1 protein and neural plasticity-related microRNAs. *Mol Neurobiol* 57: 2551–2562, 2020. doi:10.1007/s12035-020-01901-w.

13. **Strzalkowski NDJ**, **Sondergaard RE**, **Gan LS**, **Kiss ZHT.** Case studies in neuroscience: deep brain stimulation changes upper limb cortical motor maps in dystonia. *J Neurophysiol* 124: 268–273, 2020. doi:10.1152/jn.00159.2020.
14. **Wang M**, **Jia L**, **Wu X**, **Sun Z**, **Xu Z**, **Kong C**, **Ma L**, **Zhao R**, **Lu S.** Deep brain stimulation improves motor function in rats with spinal cord injury by increasing synaptic plasticity. *World Neurosurg* 140: e294–e303, 2020. doi:10.1016/j.wneu.2020.05.029.
15. **Mohan UR**, **Watrous AJ**, **Miller JF**, **Lega BC**, **Sperling MR**, **Worrell GA**, **Gross RE**, **Zaghloul KA**, **Jobst BC**, **Davis KA**, **Sheth SA**, **Stein JM**, **Das SR**, **Gorniak R**, **Wanda PA**, **Rizzuto DS**, **Kahana MJ**, **Jacobs J.** The effects of direct brain stimulation in humans depend on frequency, amplitude, and white-matter proximity. *Brain Stimul* 13: 1183–1195, 2020. doi:10.1016/j.brs.2020.05.009.
16. **Fitzgerald PB**, **Fountain S**, **Daskalakis ZJ.** A comprehensive review of the effects of rTMS on motor cortical excitability and inhibition. *Clin Neurophysiol* 117: 2584–2596, 2006. doi:10.1016/j.clinph.2006.06.712.
17. **Huang Y-Z**, **Edwards MJ**, **Rounis E**, **Bhatia KP**, **Rothwell JC.** Theta burst stimulation of the human motor cortex. *Neuron* 45: 201–206, 2005. doi:10.1016/j.neuron.2004.12.033.
18. **Suppa A**, **Huang YZ**, **Funke K**, **Ridding MC**, **Cheeran B**, **Di Lazzaro V**, **Ziemann U**, **Rothwell JC.** Ten years of theta burst stimulation in humans: established knowledge, unknowns and prospects. *Brain Stimul* 9: 323–335, 2016. doi:10.1016/j.brs.2016.01.006.
19. **Lefaucheur J-P**, **Aleman A**, **Baeken C**, **Benninger DH**, **Brunelin J**, **Di Lazzaro V**, **Filipović SR**, **Grefkes C**, **Hasan A**, **Hummel FC**, **Jääskeläinen SK**, **Langguth B**, **Leocani L**, **Londero A**, **Nardone R**, **Nguyen JP**, **Nyffeler T**, **Oliveira-Maia AJ**, **Oliviero A**, **Padberg F**, **Palm U**, **Paulus W**, **Poulet E**, **Quartarone A**, **Rachid F**, **Rektorová I**, **Rossi S**, **Sahlsten H**, **Schecklmann M**, **Szekely D**, **Ziemann U.** Evidence-based guidelines on the therapeutic use of repetitive transcranial magnetic stimulation (rTMS): an update (2014-2018). *Clin Neurophysiol* 131: 474–528, 2020 [Erratum in *Clin Neurophysiol* 131: 1168–1169, 2020]. doi:10.1016/j.clinph.2019.11.002.
20. **Lozano AM**, **Lipsman N**, **Bergman H**, **Brown P**, **Chabardes S**, **Chang JW**, **Matthews K**, **McIntyre CC**, **Schlaepfer TE**, **Schulder M**, **Temel Y**, **Volkmann J**, **Krauss JK.** Deep brain stimulation: current challenges and future directions. *Nat Rev Neurol* 15: 148–160, 2019. doi:10.1038/s41582-018-0128-2.
21. **Keller CJ**, **Huang Y**, **Herrero JL**, **Fini ME**, **Du V**, **Lado FA**, **Honey CJ**, **Mehta AD.** Induction and quantification of excitability changes in human cortical networks. *J Neurosci* 38: 5384–5398, 2018. doi:10.1523/JNEUROSCI.1088-17.2018.
22. **Bentley JN**, **Irwin ZT**, **Black SD**, **Roach ML**, **Vaden RJ**, **Gonzalez CL**, **Khan AU**, **El-Sayed GA**, **Knight RT**, **Guthrie BL**, **Walker HC.** subcortical intermittent theta-burst stimulation (iTBS) increases theta-power in dorsolateral prefrontal cortex (DLPFC). *Front Neurosci* 14: 41, 2020. doi:10.3389/fnins.2020.00041.
23. **Chung SW**, **Rogasch NC**, **Hoy KE**, **Fitzgerald PB.** The effect of single and repeated prefrontal intermittent theta burst stimulation on cortical reactivity and working memory. *Brain Stimul* 11: 566–574, 2018. doi:10.1016/j.brs.2018.01.002.
24. **Chung SW**, **Sullivan CM**, **Rogasch NC**, **Hoy KE**, **Bailey NW**, **Cash RFH**, **Fitzgerald PB.** The effects of individualised intermittent theta burst stimulation in the prefrontal cortex: a TMS-EEG study. *Hum Brain Mapp* 40: 608–627, 2019. doi:10.1002/hbm.24398.
25. **Horn MA**, **Gulberti A**, **Gülke E**, **Buhmann C**, **Gerloff C**, **Moll CKE**, **Hamel W**, **Volkmann J**, **Pötter-Nerger M.** A new stimulation mode for deep brain stimulation in Parkinson's disease: theta burst stimulation. *Mov Disord* 35: 1471–1475, 2020. doi:10.1002/mds.28083.
26. **Titiz AS**, **Hill MRH**, **Mankin EA**, **M Aghajan Z**, **Eliashiv D**, **Tchemodanov N**, **Maoz U**, **Stern J**, **Tran ME**, **Schuette P**, **Behnke E**, **Suthana NA**, **Fried I.** Theta-burst microstimulation in the human entorhinal area improves memory specificity. *eLife* 6: e29515, 2017. doi:10.7554/eLife.29515.
27. **Tse NY**, **Goldsworthy MR**, **Ridding MC**, **Coxon JP**, **Fitzgerald PB**, **Fornito A**, **Rogasch NC.** The effect of stimulation interval on plasticity following repeated blocks of intermittent theta burst stimulation. *Sci Rep* 8: 8526, 2018. doi:10.1038/s41598-018-26791-w.
28. **Yu F**, **Tang X**, **Hu R**, **Liang S**, **Wang W**, **Tian S**, **Wu Y**, **Yuan T-F**, **Zhu Y.** The after-effect of accelerated intermittent theta burst stimulation at different session intervals. *Front Neurosci* 14: 576, 2020 [Erratum in *Front Neurosci* 15: 687972, 2021]. doi:10.3389/fnins.2020.00576.
29. **Keller CJ**, **Honey CJ**, **Entz L**, **Bickel S**, **Groppe DM**, **Toth E**, **Ulbert I**, **Lado FA**, **Mehta AD.** Corticocortical evoked potentials reveal projectors and integrators in human brain networks. *J Neurosci* 34: 9152–9163, 2014. doi:10.1523/JNEUROSCI.4289-13.2014.
30. **Matsumoto R**, **Nair DR**, **Ikeda A**, **Fumuro T**, **Lapresto E**, **Mikuni N**, **Bingaman W**, **Miyamoto S**, **Fukuyama H**, **Takahashi R**, **Najm I**, **Shibasaki H**, **Lüders HO.** Parieto-frontal network in humans studied by cortico-cortical evoked potential. *Hum Brain Mapp* 33: 2856–2872, 2012. doi:10.1002/hbm.21407.
31. **Matsumoto R**, **Nair DR**, **LaPresto E**, **Bingaman W**, **Shibasaki H**, **Lüders HO.** Functional connectivity in human cortical motor system: a cortico-cortical evoked potential study. *Brain* 130: 181–197, 2007. doi:10.1093/brain/awl257.
32. **Matsumoto R**, **Nair DR**, **LaPresto E**, **Najm I**, **Bingaman W**, **Shibasaki H**, **Lüders HO.** Functional connectivity in the human language system: a cortico-cortical evoked potential study. *Brain* 127: 2316–2330, 2004. doi:10.1093/brain/awh246.
33. **Yamao Y**, **Matsumoto R**, **Kunieda T**, **Arakawa Y**, **Shibata S**, **Inano R**, **Kikuchi T**, **Sawamoto N**, **Mikuni N**, **Ikeda A**, **Fukuyama H**, **Miyamoto S.** P503: intraoperative language network monitoring by means of cortico-cortical evoked potentials. *Clin Neurophysiol* 125: S184, 2014. doi:10.1016/S1388-2457(14)50600-1.
34. **Huang Y**, **Hajnal B**, **Entz L**, **Fabó D**, **Herrero JL**, **Mehta AD**, **Keller CJ.** Intracortical dynamics underlying repetitive stimulation predicts changes in network connectivity. *J Neurosci* 39: 6122–6135, 2019. doi:10.1523/JNEUROSCI.0535-19.2019.
35. **Groppe DM**, **Bickel S**, **Dykstra AR**, **Wang X**, **Mégevand P**, **Mercier MR**, **Lado FA**, **Mehta AD**, **Honey CJ.** iELVis: an open source MATLAB toolbox for localizing and visualizing human intracranial electrode data. *J Neurosci Methods* 281: 40–48, 2017. doi:10.1016/j.jneumeth.2017.01.022.
36. **Bouton C**, **Bhagat N**, **Chandrasekaran S**, **Herrero J**, **Markowitz N**, **Espinal E**, **Kim J-W**, **Ramdeo R**, **Xu J**, **Glasser MF**, **Bickel S**, **Mehta A.** Decoding neural activity in sulcal and white matter areas of the brain to accurately predict individual finger movement and tactile stimuli of the human hand. *Front Neurosci* 15: 699631, 2021. doi:10.3389/fnins.2021.699631.
37. **Ah Sen CB**, **Fassett HJ**, **El-Sayes J**, **Turco CV**, **Hameer MM**, **Nelson AJ.** Active and resting motor threshold are efficiently obtained with adaptive threshold hunting. *PLoS One* 12: e0186007, 2017. doi:10.1371/journal.pone.0186007.
38. **Rossini PM**, **Burke D**, **Chen R**, **Cohen LG**, **Daskalakis Z**, **Di Iorio R**, **Di Lazzaro V**, **Ferreri F**, **Fitzgerald PB**, **George MS**, **Hallett M**, **Lefaucheur JP**, **Langguth B**, **Matsumoto H**, **Miniussi C**, **Nitsche MA**, **Pascual-Leone A**, **Paulus W**, **Rossi S**, **Rothwell JC**, **Siebner HR**, **Ugawa Y**, **Walsh V**, **Ziemann U.** Non-invasive electrical and magnetic stimulation of the brain, spinal cord, roots and peripheral nerves: basic principles and procedures for routine clinical and research application. An updated report from an I.F.C.N. Committee. *Clin Neurophysiol* 126: 1071–1107, 2015. doi:10.1016/j.clinph.2015.02.001.
39. **Rothwell JC**, **Hallett M**, **Berardelli A**, **Eisen A**, **Rossini P**, **Paulus W.** Magnetic stimulation: motor evoked potentials. The International Federation of Clinical Neurophysiology. *Electroencephalogr Clin Neurophysiol Suppl* 52: 97–103, 1999.
40. **Goldsworthy MR**, **Pitcher JB**, **Ridding MC.** The application of spaced theta burst protocols induces long-lasting neuroplastic changes in the human motor cortex. *Eur J Neurosci* 35: 125–134, 2012. doi:10.1111/j.1460-9568.2011.07924.x.
41. **Kelley R**, **Flouty O**, **Emmons EB**, **Kim Y**, **Kingyon J**, **Wessel JR**, **Oya H**, **Greenlee JD**, **Narayanan NS.** A human prefrontal-subthalamic circuit for cognitive control. *Brain* 141: 205–216, 2018. doi:10.1093/brain/awx300.
42. **Scangos KW**, **Carter CS**, **Gurkoff G**, **Zhang L**, **Shahlaie K.** A pilot study of subthalamic theta frequency deep brain stimulation for cognitive dysfunction in Parkinson's disease. *Brain Stimul* 11: 456–458, 2018. doi:10.1016/j.brs.2017.11.014.
43. **Entz L**, **Tóth E**, **Keller CJ**, **Bickel S**, **Groppe DM**, **Fabó D**, **Kozák LR**, **Erőss L**, **Ulbert I**, **Mehta AD.** Evoked effective connectivity of the human neocortex. *Hum Brain Mapp* 35: 5736–5753, 2014. doi:10.1002/hbm.22581.
44. **Mégevand P**, **Groppe DM**, **Bickel S**, **Mercier MR**, **Goldfinger MS**, **Keller CJ**, **Entz L**, **Mehta AD.** The hippocampus and amygdala are integrators of neocortical influence: a corticocortical evoked

potential study. *Brain Connect* 7: 648–660, 2017. doi:10.1089/brain.2017.0527.
45. **Matsuzaki N**, **Juhász C**, **Asano E.** Cortico-cortical evoked potentials and stimulation-elicited gamma activity preferentially propagate from lower- to higher-order visual areas. *Clin Neurophysiol* 124: 1290–1296, 2013. doi:10.1016/j.clinph.2013.02.007.
46. **Enatsu R**, **Kubota Y**, **Kakisaka Y**, **Bulacio J**, **Piao Z**, **O'Connor T**, **Horning K**, **Mosher J**, **Burgess RC**, **Bingaman W**, **Nair DR.** Reorganization of posterior language area in temporal lobe epilepsy: a cortico-cortical evoked potential study. *Epilepsy Res* 103: 73–82, 2013. doi:10.1016/j.eplepsyres.2012.07.008.
47. **Oostenveld R**, **Fries P**, **Maris E**, **Schoffelen J-M.** FieldTrip: open source software for advanced analysis of MEG, EEG, and invasive electrophysiological data. *Comput Intell Neurosci* 2011: 156869, 2011. doi:10.1155/2011/156869.
48. **Nunez PL**, **Silberstein RB**, **Shi Z**, **Carpenter MR**, **Srinivasan R**, **Tucker DM**, **Doran SM**, **Cadusch PJ**, **Wijesinghe RS.** EEG coherency II: experimental comparisons of multiple measures. *Clin Neurophysiol* 110: 469–486, 1999. doi:10.1016/s1388-2457(98)00043-1.
49. **Ríos-Herrera WA**, **Olguín-Rodríguez PV**, **Arzate-Mena JD**, **Corsi-Cabrera M**, **Escalona J**, **Marín-García A**, **Ramos-Loyo J**, **Rivera AL**, **Rivera-López D**, **Zapata-Berruecos JF**, **Müller MF.** The influence of EEG references on the analysis of spatio-temporal interrelation patterns. *Front Neurosci* 13: 941, 2019. doi:10.3389/fnins.2019.00941.
50. **Zaveri HP**, **Duckrow RB**, **Spencer SS.** On the use of bipolar montages for time-series analysis of intracranial electroencephalograms. *Clin Neurophysiol* 117: 2102–2108, 2006. doi:10.1016/j.clinph.2006.05.032.
51. **Mitra PP**, **Pesaran B.** Analysis of dynamic brain imaging data. *Biophys J* 76: 691–708, 1999. doi:10.1016/S0006-3495(99)77236-X.
52. **Bastos AM**, **Schoffelen J-M.** A tutorial review of functional connectivity analysis methods and their interpretational pitfalls. *Front Syst Neurosci* 9: 175, 2015. doi:10.3389/fnsys.2015.00175.
53. **Barone J**, **Rossiter HE.** Understanding the role of sensorimotor beta oscillations. *Front Syst Neurosci* 15: 655886, 2021. doi:10.3389/fnsys.2021.655886.
54. **Sherman MA**, **Lee S**, **Law R**, **Haegens S**, **Thorn CA**, **Hämäläinen MS**, **Moore CI**, **Jones SR.** Neural mechanisms of transient neocortical beta rhythms: converging evidence from humans, computational modeling, monkeys, and mice. *Proc Natl Acad Sci USA* 113: E4885–E4894, 2016. doi:10.1073/pnas.1604135113.
55. **Chandrasekaran S**, **Nanivadekar AC**, **McKernan G**, **Helm ER**, **Boninger ML**, **Collinger JL**, **Gaunt RA**, **Fisher LE.** Sensory restoration by epidural stimulation of the lateral spinal cord in upper-limb amputees. *eLife* 9: e54349, 2020 [Erratum in *eLife* 10: e72438, 2021]. doi:10.7554/eLife.54349.
56. **Bikson M**, **Dmochowski J**, **Rahman A.** The "quasi-uniform" assumption in animal and computational models of non-invasive electrical stimulation. *Brain Stimul* 6: 704–705, 2013. doi:10.1016/j.brs.2012.11.005.
57. **Zanos S**, **Rembado I**, **Chen D**, **Fetz EE.** Phase-locked stimulation during cortical beta oscillations produces bidirectional synaptic plasticity in awake monkeys. *Curr Biol* 28: 2515–2526.e4, 2018. doi:10.1016/j.cub.2018.07.009.
58. **Laviolette L**, **Niérat M-C**, **Hudson AL**, **Raux M**, **Allard E**, **Similowski T.** The supplementary motor area exerts a tonic excitatory influence on corticospinal projections to phrenic motoneurons in awake humans. *PLoS One* 8: e62258, 2013. doi:10.1371/journal.pone.0062258.
59. **Oberman L**, **Edwards D**, **Eldaief M**, **Pascual-Leone A.** Safety of theta burst transcranial magnetic stimulation: a systematic review of the literature. *J Clin Neurophysiol* 28: 67–74, 2011. doi:10.1097/WNP.0b013e318205135f.
60. **Mina F**, **Benquet P**, **Pasnicu A**, **Biraben A**, **Wendling F.** Modulation of epileptic activity by deep brain stimulation: a model-based study of frequency-dependent effects. *Front Comput Neurosci* 7: 94, 2013. doi:10.3389/fncom.2013.00094.
61. **Stypulkowski PH**, **Stanslaski SR**, **Giftakis JE.** Modulation of hippocampal activity with fornix deep brain stimulation. *Brain Stimul* 10: 1125–1132, 2017. doi:10.1016/j.brs.2017.09.002.
62. **Elias GJB**, **Namasivayam AA**, **Lozano AM.** Deep brain stimulation for stroke: current uses and future directions. *Brain Stimul* 11: 3–28, 2018. doi:10.1016/j.brs.2017.10.005.
63. **Benazzouz A**, **Hamani , C.** Mechanisms of deep brain stimulation. In: *Fundamentals and Clinics of Deep Brain Stimulation: an Interdisciplinary Approach*, edited by Temel Y, Leentjens AFG, de Bie RMA, Chabardes S, Fasano A. Cham, Switzerland: Springer International Publishing, 2020, p. 29–37.
64. **Herrington TM**, **Cheng JJ**, **Eskandar EN.** Mechanisms of deep brain stimulation. *J Neurophysiol* 115: 19–38, 2016 [Erratum in *J Neurophysiol* 123: 1277, 2020]. doi:10.1152/jn.00281.2015.
65. **Stoney SD**, **Thompson WD**, **Asanuma H.** Excitation of pyramidal tract cells by intracortical microstimulation: effective extent of stimulating current. *J Neurophysiol* 31: 659–669, 1968. doi:10.1152/jn.1968.31.5.659.
66. **Tehovnik EJ**, **Tolias AS**, **Sultan F**, **Slocum WM**, **Logothetis NK.** Direct and indirect activation of cortical neurons by electrical microstimulation. *J Neurophysiol* 96: 512–521, 2006. doi:10.1152/jn.00126.2006.
67. **Wagner T**, **Eden U**, **Fregni F**, **Valero-Cabre A**, **Ramos-Estebanez C**, **Pronio-Stelluto V**, **Grodzinsky A**, **Zahn M**, **Pascual-Leone A.** Transcranial magnetic stimulation and brain atrophy: a computer-based human brain model study. *Exp Brain Res* 186: 539–550, 2008. doi:10.1007/s00221-007-1258-8.
68. **Wilson MT**, **Fulcher BD**, **Fung PK**, **Robinson PA**, **Fornito A**, **Rogasch NC.** Biophysical modeling of neural plasticity induced by transcranial magnetic stimulation. *Clin Neurophysiol* 129: 1230–1241, 2018. doi:10.1016/j.clinph.2018.03.018.
69. **Paus T**, **Jech R**, **Thompson CJ**, **Comeau R**, **Peters T**, **Evans AC.** Transcranial magnetic stimulation during positron emission tomography: a new method for studying connectivity of the human cerebral cortex. *J Neurosci* 17: 3178–3184, 1997. doi:10.1523/JNEUROSCI.17-09-03178.1997.
70. **Bergmann TO**, **Varatheeswaran R**, **Hanlon CA**, **Madsen KH**, **Thielscher A**, **Siebner HR.** Concurrent TMS-fMRI for causal network perturbation and proof of target engagement. *NeuroImage* 237: 118093, 2021. doi:10.1016/j.neuroimage.2021.118093.
71. **Farzan F**, **Vernet M**, **Shafi MMD**, **Rotenberg A**, **Daskalakis ZJ**, **Pascual-Leone A.** Characterizing and modulating brain circuitry through transcranial magnetic stimulation combined with electroencephalography. *Front Neural Circuits* 10: 73, 2016. doi:10.3389/fncir.2016.00073.
72. **Di Lazzaro V**, **Pilato F**, **Saturno E**, **Oliviero A**, **Dileone M**, **Mazzone P**, **Insola A**, **Tonali PA**, **Ranieri F**, **Huang YZ**, **Rothwell JC.** Theta-burst repetitive transcranial magnetic stimulation suppresses specific excitatory circuits in the human motor cortex. *J Physiol* 565: 945–950, 2005. doi:10.1113/jphysiol.2005.087288.
73. **Terao Y**, **Ugawa Y.** Basic mechanisms of TMS. *J Clin Neurophysiol* 19: 322–343, 2002. doi:10.1097/00004691-200208000-00006.
74. **Parvizi J**, **Kastner S.** Promises and limitations of human intracranial electroencephalography. *Nat Neurosci* 21: 474–483, 2018. doi:10.1038/s41593-018-0108-2.
75. **Bestmann S**, **Baudewig J**, **Siebner HR**, **Rothwell JC**, **Frahm J.** BOLD MRI responses to repetitive TMS over human dorsal premotor cortex. *NeuroImage* 28: 22–29, 2005. doi:10.1016/j.neuroimage.2005.05.027.
76. **Edgley SA**, **Eyre JA**, **Lemon RN**, **Miller S.** Excitation of the corticospinal tract by electromagnetic and electrical stimulation of the scalp in the macaque monkey. *J Physiol* 425: 301–320, 1990. doi:10.1113/jphysiol.1990.sp018104.
77. **Kumar R**, **Chen R**, **Ashby P.** Safety of transcranial magnetic stimulation in patients with implanted deep brain stimulators. *Mov Disord* 14: 157–158, 1999. doi:10.1002/1531-8257(199901)14:1<157::AID-MDS1027>3.0.CO;2-U.
78. **Rossi S**, **Antal A**, **Bestmann S**, **Bikson M**, **Brewer C**, **Brockmöller J**, et al. Safety and recommendations for TMS use in healthy subjects and patient populations, with updates on training, ethical and regulatory issues: expert guidelines. *Clin Neurophysiol* 132: 269–306, 2021. doi:10.1016/j.clinph.2020.10.003.
79. **Kühn AA**, **Brandt SA**, **Kupsch A**, **Trottenberg T**, **Brocke J**, **Irlbacher K**, **Schneider GH**, **Meyer B-U.** Comparison of motor effects following subcortical electrical stimulation through electrodes in the globus pallidus internus and cortical transcranial magnetic stimulation. *Exp Brain Res* 155: 48–55, 2004. doi:10.1007/s00221-003-1707-y.
80. **So RQ**, **McConnell GC**, **Grill WM.** Frequency-dependent, transient effects of subthalamic nucleus deep brain stimulation on

methamphetamine-induced circling and neuronal activity in the hemiparkinsonian rat. *Behav Brain Res* 320: 119–127, 2017. doi:10.1016/j.bbr.2016.12.003.

81. **Su D**, **Chen H**, **Hu W**, **Liu Y**, **Wang Z**, **Wang X**, **Liu G**, **Ma H**, **Zhou J**, **Feng T.** Frequency-dependent effects of subthalamic deep brain stimulation on motor symptoms in Parkinson's disease: a meta-analysis of controlled trials. *Sci Rep* 8: 14456, 2018. doi:10.1038/s41598-018-32161-3.
82. **Ridding MC**, **Ziemann U.** Determinants of the induction of cortical plasticity by non-invasive brain stimulation in healthy subjects. *J Physiol* 588: 2291–2304, 2010. doi:10.1113/jphysiol.2010.190314.
83. **Schutter DJLG**, **Hortensius R.** Brain oscillations and frequency-dependent modulation of cortical excitability. *Brain Stimul* 4: 97–103, 2011. doi:10.1016/j.brs.2010.07.002.
84. **Lendner JD**, **Helfrich RF**, **Mander BA**, **Romundstad L**, **Lin JJ**, **Walker MP**, **Larsson PG**, **Knight RT.** An electrophysiological marker of arousal level in humans. *eLife* 9: e55092, 2020. doi:10.7554/eLife.55092.
85. **Stolk A**, **Brinkman L**, **Vansteensel MJ**, **Aarnoutse E**, **Leijten FS**, **Dijkerman CH**, **Knight RT**, **de Lange FP**, **Toni I.** Electrocorticographic dissociation of alpha and beta rhythmic activity in the human sensorimotor system. *eLife* 8: e48065, 2019. doi:10.7554/eLife.48065.
86. **Cole EJ**, **Stimpson KH**, **Bentzley BS**, **Gulser M**, **Cherian K**, **Tischler C**, **Nejad R**, **Pankow H**, **Choi E**, **Aaron H**, **Espil FM**, **Pannu J**, **Xiao X**, **Duvio D**, **Solvason HB**, **Hawkins J**, **Guerra A**, **Jo B**, **Raj KS**, **Phillips AL**, **Barmak F**, **Bishop JH**, **Coetzee JP**, **DeBattista C**, **Keller J**, **Schatzberg AF**, **Sudheimer KD**, **Williams NR.** Stanford accelerated intelligent neuromodulation therapy for treatment-resistant depression. *Am J Psychiatry* 177: 716–726, 2020. doi:10.1176/appi.ajp.2019.19070720.
87. **Solomon EA**, **Sperling MR**, **Sharan AD**, **Wanda PA**, **Levy DF**, **Lyalenko A**, **Pedisich I**, **Rizzuto DS**, **Kahana MJ.** Theta-burst stimulation entrains frequency-specific oscillatory responses. *Brain Stimul* 14: 1271–1284, 2021. doi:10.21203/rs.3.rs-308421/v1.
88. **Jensen O**, **Goel P**, **Kopell N**, **Pohja M**, **Hari R**, **Ermentrout B.** On the human sensorimotor-cortex beta rhythm: sources and modeling. *Neuroimage* 26: 347–355, 2005. doi:10.1016/j.neuroimage.2005.02.008.
89. **Olson JD**, **Caldwell D**, **Wander JD**, **Zanos S**, **Sata D**, **Su D**, **Cronin J**, **Collins K**, **Wu J**, **Casimo K**, **Johnson L**, **Weaver K**, **Fetz EE**, **Rao RPN**, **Ojemann JG.** Dose dependent enhancement of cortico-cortical evoked potentials during beta-oscillation triggered direct electrical stimulation of human cortex. *NSF Center for Sensorimotor Neural Engineering Annual Meeting*. Seattle, WA, April 11–13, 2016.
90. **Lockyer EJ**, **Compton CT**, **Forman DA**, **Pearcey GE**, **Button DC**, **Power KE.** Moving forward: methodological considerations for assessing corticospinal excitability during rhythmic motor output in humans. *J Neurophysiol* 126: 181–194, 2021. doi:10.1152/jn.00027.2021.
91. **Suthana N**, **Haneef Z**, **Stern J**, **Mukamel R**, **Behnke E**, **Knowlton B**, **Fried I.** Memory enhancement and deep-brain stimulation of the entorhinal area. *N Engl J Med* 366: 502–510, 2012. doi:10.1056/NEJMoa1107212.
92. **Salinas MR.** Common programming strategies for deep brain stimulation. In: *Deep Brain Stimulation: A Case-based Approach*, edited by Chitnis S, Khemani P, Okun MS**.** New York: Oxford University Press, 2020, p. 3–8.
93. **Seo H**, **Jun SC.** Multi-scale computational models for electrical brain stimulation. *Front Hum Neurosci* 11: 515, 2017. doi:10.3389/fnhum.2017.00515.
94. **Darmani G**, **Bergmann TO**, **Zipser C**, **Baur D**, **Müller-Dahlhaus F**, **Ziemann U.** Effects of antiepileptic drugs on cortical excitability in humans: a TMS-EMG and TMS-EEG study. *Hum Brain Mapp* 40: 1276–1289, 2019. doi:10.1002/hbm.24448.
95. **Ziemann U**, **Lönnecker S**, **Steinhoff BJ**, **Paulus W.** Effects of antiepileptic drugs on motor cortex excitability in humans: a transcranial magnetic stimulation study. *Ann Neurol* 40: 367–378, 1996. doi:10.1002/ana.410400306.